

Observational signatures of the parametric amplification of gravitational waves during reheating after inflation

Sachiko Kuroyanagi¹, Chunshan Lin^{2,3}, Misao Sasaki², Shinji Tsujikawa⁴

¹*Department of Physics, Nagoya University, Chikusa, Nagoya 464-8602, Japan*

²*Yukawa Institute for Theoretical Physics, Kyoto University, 606-8502, Kyoto, Japan*

³*Institute of Theoretical Physics, Faculty of Physics, University of Warsaw, ul. Pasteura 5, Warsaw, Poland*

⁴*Department of Physics, Faculty of Science, Tokyo University of Science, 1-3, Kagurazaka, Shinjuku-ku, Tokyo 162-8601, Japan*

(Dated: March 13, 2022)

We study the evolution of Gravitational Waves (GWs) during and after inflation as well as the resulting observational consequences in a Lorentz-violating massive gravity theory with one scalar (inflaton) and two tensor degrees of freedom. We consider two explicit examples of the tensor mass m_g that depends either on the inflaton field ϕ or on its time derivative $\dot{\phi}$, both of which lead to parametric excitations of GWs during reheating after inflation. The first example is Starobinsky's R^2 inflation model with a ϕ -dependent m_g and the second is a low-energy-scale inflation model with a $\dot{\phi}$ -dependent m_g . We compute the energy density spectrum $\Omega_{\text{GW}}(k)$ today of the GW background. In the Starobinsky's model, we show that the GWs can be amplified up to the detectable ranges of both CMB and DECIGO, but the bound from the big bang nucleosynthesis is quite tight to limit the growth. In low-scale inflation with a fast transition to the reheating stage driven by the potential $V(\phi) = M^2 \phi^2/2$ around $\phi \approx M_{\text{pl}}$ (where M_{pl} is the reduced Planck mass), we find that the peak position of $\Omega_{\text{GW}}(k)$ induced by the parametric resonance can reach the sensitivity region of advanced LIGO for the Hubble parameter of order 1 GeV at the end of inflation. Thus, our massive gravity scenario offers exciting possibilities for probing the physics of primordial GWs at various different frequencies.

I. INTRODUCTION

The inflationary paradigm successfully addresses several problems of the big-bang cosmology [1, 2]. But most importantly it gives a unique mechanism to generate primordial cosmological perturbations that give rise to the structure of the Universe [3, 4]. In the standard picture, the cosmic acceleration is driven by the potential energy of a scalar degree of freedom ϕ (dubbed “inflaton”). The quantum fluctuations of the inflaton, which are stretched over the scales greater than the Hubble radius, are the source of the primordial scalar-type curvature perturbation [3, 5]. The amplitude and the spectral index of the scalar perturbation are now tightly constrained by the Planck CMB measurements [6].

Besides the scalar perturbation, the tensor perturbation is also generated during inflation [7]¹. In the single-field scenario with the massless tensor mode, the tensor-to-scalar ratio $r = \mathcal{P}_T(k)/\mathcal{P}_R(k)$ is related to the slow-roll parameter $\epsilon (= -\dot{H}/H^2)$, as $r = 16\epsilon$ [8]. Since we require the condition $\epsilon \ll 1$ for realizing inflation, the amplitude of the tensor perturbation is smaller than that of the scalar perturbation. The CMB observations so far have placed only the upper bound of the tensor-to-scalar ratio, as $r < 0.11$ (95 % CL) [6].

Depending on models of inflation, the values of ϵ associated with the observed CMB scale are different. In

the so-called small-field inflation where the variation of ϕ during inflation does not exceed the reduced Planck mass $M_{\text{pl}} = 2.435 \times 10^{18}$ GeV, we have $\epsilon \lesssim 10^{-4}$ [9–11]. In Starobinsky's model [1], $\epsilon \sim 10^{-4}$ [12], so it marginally belongs to small-field inflation. The next target of CMB B-mode measurements like LiteBIRD [13] and the ground-based Stage-4 effort [14] is the detection of primordial GWs with r down to the order of 10^{-3} .

There are inflationary models in which $\epsilon \ll 10^{-4}$, e.g., those arising from string theory [15]. In such models, it is usually believed that the detection of primordial GWs is impossible even with future high-precision CMB B-mode measurements. However, this is not necessarily the case if the tensor perturbation is subject to some growth after inflation. Indeed, there are models in which the existence of a time-dependent tensor mass leads to the amplification of GWs during the reheating stage after inflation [16]².

The massive gravity scenario studied in Ref. [16], which was originally advocated in Refs. [18, 19], is constructed under the internal $SO(3)$ symmetry $\phi^i \rightarrow \Lambda^i_j \phi^j$, and $\phi^i \rightarrow \phi^i + \Xi^i(\phi^0)$, where Ξ^i is a general function of its argument. The tensor modes acquire a mass due to the non-trivial vacuum expectation value of these four scalar fields $\phi^\mu = x^\mu$. This property differs from the original Fierz-Pauli theory [20] and its nonlinear extension [21]

¹ Throughout this paper, by “scalar, vector, and tensor” we mean those with respect to the symmetry of 3-space.

² There are also models in which the anisotropic stress of scalar fields work as a source term for the production of GWs during reheating [17]. In this paper, we will not consider such a scenario.

in which the scalar field configuration respects Poincare symmetry. The internal symmetry $\phi^i \rightarrow \phi^i + \Xi^i(\phi^0)$ forbids the propagation of vector modes [18, 19], so we are left with only three dynamical degrees of freedom: one scalar mode and two tensor modes.³

We minimally extend our inflationary scenario by adding this tensor mass m_g into our theory, and identify the scalar mode with the inflaton scalar field ϕ [16]. Since the scalar mode does not give rise to a ghost state, our theory is free from the Higuchi bound [22], which is always an issue in cosmology for theories that respect de Sitter symmetry. Further we impose the global scaling symmetry $\phi^i \rightarrow \lambda\phi^i$, which guarantees the non-dynamical nature of ϕ^i in the cosmological background [16, 23].

Generally the tensor mass m_g can depend on the field ϕ or its time derivative $\dot{\phi}$. To recover the local Lorentz-invariance after reheating, we require that m_g eventually vanishes. The ϕ -dependent tensor mass leads to the parametric resonant amplification of GWs at the early stage of reheating [24, 25] due to coherent oscillations of the inflaton around the potential minimum [16].

The parametric amplification in our massive gravity theory will give rise to several distinct observational signatures in CMB and direct measurements of GWs. Even for small-field inflation in which the slow-roll parameter ϵ is very small, $\epsilon \ll 10^{-4}$, the GWs can be amplified to the detectable level in near-future CMB experiments ($r \gtrsim 10^{-3}$). Moreover, this parametric excitation is at work down to scales smaller than the Hubble radius at the onset of reheating. This may offer the possibility of detecting GWs in direct measurements such as Advanced-LIGO (A-LIGO) [26] and DECIGO [27].

In this paper, we make a thorough, quantitative analysis of the parametric resonance in two typical, explicit models of the tensor mass term. We consider small-field inflationary models with two different forms of m_g that depends on either ϕ or $\dot{\phi}$ and compute the primordial tensor power spectrum \mathcal{P}_T after the amplification as well as the today's energy density spectrum $\Omega_{\text{GW}}(k)$ of the GW background. In Starobinsky's model with a ϕ -dependent m_g , we will discuss the possibility of amplifying GWs at the detectable level in both CMB and DECIGO measurements. In this model, however, the peak position of $\Omega_{\text{GW}}(k)$ induced by the parametric excitation of GWs is at frequency much larger than the frequency bands of A-LIGO.

We will also study a low-scale inflation model with a $\dot{\phi}$ -dependent m_g . We consider an inflationary scenario where a fast transition from a nearly flat potential to the reheating stage driven by the potential $V(\phi) = M^2\phi^2/2$

occurs around ϕ of the order of M_{pl} . For the potentials where the field value ϕ_{end} at the end of inflation is much smaller than M_{pl} the parametric resonance is less efficient, so we focus on the models with $\phi_{\text{end}} = \mathcal{O}(M_{\text{pl}})$. We will show that, as the Hubble expansion rate H_i at the onset of reheating gets smaller, the peak position of $\Omega_{\text{GW}}(k)$ shifts toward smaller frequencies. For $H_i \lesssim 1$ GeV, the peak may reach the sensitivity band of A-LIGO.

This paper is organized as follows. In Sec. II, we briefly review the Lorentz-violating massive gravity model and present explicit forms of the tensor mass that lead to the amplification of GWs during reheating. In Sec. III, we derive the primordial tensor power spectrum generated right after the end of inflation. In Sec. IV, we discuss how the parametric resonance of GWs occurs during reheating for two different tensor masses. In Secs. V and VI we numerically calculate the GW power spectra after the amplification in Starobinsky's model with a ϕ -dependent m_g and in a low-scale inflation model with a $\dot{\phi}$ -dependent m_g , respectively. In Sec. VII, we compute the today's power spectrum of the GW background in the two models and discuss the possibility of detecting the GWs in direct measurements. Sec. VIII is devoted to conclusions.

II. MASSIVE TENSOR GRAVITY AND INFLATION

The Lorentz-violating massive gravity theory proposed in Refs. [18, 19] contains four scalar Goldstone fields ϕ^0 and ϕ^i respecting the internal symmetry

$$\phi^i \rightarrow \Lambda^i_j \phi^j, \quad \phi^0 \rightarrow \phi^0 + \Xi^i(\phi^0), \quad (2.1)$$

where Ξ^i is a general function of its argument. The tensor mass arises from the scalar fields' non-trivial vacuum expectation values (VEVs)

$$\phi^0 = t, \quad \phi^i = x^i. \quad (2.2)$$

At the level of lowest dimensional operators, there are two ingredients respecting the internal symmetry [18],

$$X = g^{\mu\nu} \partial_\mu \phi^0 \partial_\nu \phi^0, \quad (2.3)$$

$$Z^{ij} = g^{\mu\nu} \partial_\mu \phi^i \partial_\nu \phi^j - \frac{g^{\mu\nu} \partial_\mu \phi^0 \partial_\nu \phi^i g^{\lambda\rho} \partial_\lambda \phi^0 \partial_\rho \phi^j}{X}, \quad (2.4)$$

where $g^{\mu\nu}$ is the metric tensor. In the gauge where the scalar field values are fixed at its VEVs, $\phi^\mu = x^\mu$, these quantities reduce to $X = -N^{-2}$ and $Z^{ij} = h^{ij}$, respectively, where h^{ij} is the three-dimensional induced metric in terms of the Arnowitt-Deser-Misner (ADM) decomposition.

The above model motivates us to consider a model that minimally modifies gravity when applied to cosmology. We first identify ϕ^0 with the inflaton, $\phi = \phi^0$. Then we introduce a traceless tensor constructed from Z^{ij} , as [28]

$$\bar{\delta}Z^{ij} \equiv Z^{ij} - \frac{3\delta_{kl}Z^{ik}Z^{jl}}{Z}, \quad (2.5)$$

³ Throughout the paper, we avoid using the terminology ‘‘graviton’’ for the description of our tensor modes because the graviton, as a massive spin 2 particle, must have five propagating degrees of freedom due to the Poincare symmetry in the Minkowskian space-time, which is broken in our model.

where $Z \equiv Z^{ij}\delta_{ij}$, and consider the action [16, 23]

$$S = \int d^4x \sqrt{-g} \left[\frac{M_{\text{pl}}^2}{2} R - \frac{1}{2} g^{\mu\nu} \partial_\mu \phi \partial_\nu \phi - V(\phi) - \frac{9}{8} M_{\text{pl}}^2 m_g^2 \frac{(\bar{\delta} Z^{ij})^2}{Z^2} \right], \quad (2.6)$$

where R is the four-dimensional Ricci scalar, $V(\phi)$ is the potential of the scalar field ϕ , m_g is the tensor mass dynamically changing in time, and $(\bar{\delta} Z^{ij})^2 \equiv \delta_{ik}\delta_{jl}\bar{\delta} Z^{ij}\bar{\delta} Z^{kl}$. In addition to the symmetry (2.1), the above action has an additional global symmetry,

$$\phi^i \rightarrow \lambda \phi^i, \quad (2.7)$$

where λ is a constant.⁴

On the flat Friedmann-Lemaître-Robertson-Walker (FLRW) background described by the line-element $ds^2 = -dt^2 + a^2(t)\delta_{ij}dx^i dx^j$, where $a(t)$ is the time-dependent scale factor, the rescaling symmetry (2.7) guarantees that the VEVs of ϕ^i may be identified with the comoving coordinates $\phi^i = x^i$, and ϕ^i remains non-dynamical [16, 23]. The dynamical equations of motion are given by

$$3M_{\text{pl}}^2 H^2 = \frac{1}{2} \dot{\phi}^2 + V, \quad (2.8)$$

$$2M_{\text{pl}}^2 \dot{H} = -\dot{\phi}^2, \quad (2.9)$$

$$\ddot{\phi} + 3H\dot{\phi} + V_{,\phi} = 0, \quad (2.10)$$

where an overdot represents a derivative with respect to t , $H \equiv \dot{a}/a$ is the Hubble parameter, and $V_{,\phi} \equiv dV/d\phi$. Note that the tensor mass term in the action (2.6) does not affect the background equations of motion.

As usual, since the inflaton evolves slowly along a nearly flat potential during inflation, Eqs. (2.8) and (2.10) approximately reduce to $3M_{\text{pl}}^2 H^2 \simeq V$ and $3H\dot{\phi} \simeq -V_{,\phi}$, respectively. We define the slow-roll parameter,

$$\epsilon \equiv -\frac{\dot{H}}{H^2} \simeq \frac{3\dot{\phi}^2}{2V} \simeq \epsilon_V, \quad \epsilon_V \equiv \frac{M_{\text{pl}}^2}{2} \left(\frac{V_{,\phi}}{V} \right)^2, \quad (2.11)$$

which is much smaller than unity during inflation.

We assume that the tensor mass m_g depends on either ϕ or $\dot{\phi}$. For the so-called broad parametric resonance to occur during the stage when the inflaton undergoes damped oscillations, we require that m_g^2 is larger than H^2 [25]. On the other hand, if $m_g^2 \gtrsim H^2$ during inflation, the tensor perturbation is subject to strong suppression by the heavy tensor mass (see e.g., Refs. [29]). To avoid this suppression, we consider the case in which $m_g^2/H^2 \ll 1$ during most stage of inflation and m_g^2/H^2 quickly grows to the value larger than the order of unity around the

end of inflation. It is possible to realize such changes for the following two examples:

$$(i) \quad m_g^2(\phi) = \lambda \phi^2 e^{-b(\phi/M_{\text{pl}})^n}, \quad (2.12)$$

$$(ii) \quad m_g^2(\dot{\phi}) = \mu \frac{\dot{\phi}^2}{M_{\text{pl}}^2}, \quad (2.13)$$

where λ, b, n, μ are positive dimensionless constants. For the potential with a minimum at $\phi = 0$, the tensor mass in the case (i) rapidly approaches 0 as the inflaton decays to radiation. This property also persists in the case of (ii). Hence the current observational bounds of the tensor mass [30] can be safely satisfied for the above two choices of m_g^2 .

In the case (i), if inflation occurs in the region where ϕ is larger than M_{pl} , the exponential factor in Eq. (2.12) with $b = \mathcal{O}(1)$ can suppress $m_g^2(\phi)$ so that $m_g^2(\phi)/H^2 \ll 1$ during inflation. The ratio $m_g^2(\phi)/H^2$ can grow with the decrease of ϕ toward the end of inflation, so this allows the possibility to realize the broad parametric resonance driven by the oscillating tensor mass squared $m_g^2(\phi) \simeq \lambda \phi^2$ around $\phi = 0$.

In the case (ii), the ratio between $m_g^2(\dot{\phi}^2)$ and H^2 during inflation can be estimated as

$$\frac{m_g^2(\dot{\phi}^2)}{H^2} \simeq 2\mu\epsilon, \quad (2.14)$$

which is smaller than unity for $\mu\epsilon \ll 1$. The slow-roll parameter ϵ grows to the order of unity by the end of inflation, so the ratio $m_g^2(\dot{\phi}^2)/H^2$ becomes larger than unity for $\mu \gtrsim 1$ around the onset of reheating. Thus, the broad parametric resonance can occur for $\mu \gg 1$.

III. PRIMORDIAL POWER SPECTRA GENERATED DURING INFLATION

We consider a linearly perturbed line-element on the flat FLRW background, as

$$ds^2 = -(1 + 2\alpha)dt^2 + 2a(t) (\beta_{|i} + S_i) dt dx^i + a^2(t) [(1 + 2\psi)\delta_{ij} + 2E_{|ij} + 2F_{i|j} + \gamma_{ij}] dx^i dx^j, \quad (3.1)$$

where the subscript $|i$ represents a three-dimensional covariant derivative, α, β, ψ, E are scalar metric perturbations, S_i, F_i are vector perturbations satisfying the transverse conditions $S_i{}^{|i} = 0, F_i{}^{|i} = 0$, and γ_{ij} is the tensor perturbation obeying the transverse and traceless conditions $\gamma_{ij}{}^{|j} = 0, \gamma_i{}^i = 0$. Since the vector perturbation does not propagate in our massive gravity theory due to the internal symmetry (2.7) [16, 23], we will consider the propagation of scalar and tensor perturbations in the following.

⁴ It may be noted that if $m_g^2 = m_g^2(X)$ and $V = 0$ at tree level, the action becomes shift symmetric, $\phi^\mu \rightarrow \phi^\mu + \text{constant}$.

A. Scalar power spectrum

At the level of linear cosmological perturbations, the tensor mass term on the r.h.s. of Eq. (2.6) does not modify the dynamics of scalar perturbations. We define the curvature perturbation, as $\mathcal{R} = \psi - H\delta\phi/\dot{\phi}$, where $\delta\phi$ is the perturbation of ϕ . Since $\delta\phi = 0$ in the unitary gauge (2.2), \mathcal{R} is equivalent to ψ . The primordial power spectrum of \mathcal{R} generated right after the end of inflation is given by [8]

$$\mathcal{P}_{\mathcal{R}} = \frac{H^2}{8\pi^2\epsilon M_{\text{pl}}^2} \Big|_{k=aH}, \quad (3.2)$$

where k is the comoving wavenumber and ϵ is given by Eq. (2.11). The power spectrum (3.2) should be evaluated at the Hubble horizon crossing ($k = aH$) during inflation. The scalar spectral index is

$$n_s - 1 \equiv \frac{d \ln \mathcal{P}_{\mathcal{R}}}{d \ln k} \Big|_{k=aH} = -6\epsilon_V + 2\eta_V, \quad (3.3)$$

where ϵ_V is defined in Eq. (2.11), and

$$\eta_V \equiv \frac{M_{\text{pl}}^2 V_{,\phi\phi}}{V}. \quad (3.4)$$

From the CMB observations, the amplitude of the primordial scalar power spectrum (3.2) is constrained to be $\mathcal{P}_{\mathcal{R}} \simeq 2.2 \times 10^{-9}$ for the perturbation which crossed the Hubble radius about the number of e-folding $N = 55$ before the end of inflation [6]. This implies that the Hubble parameter during inflation (denoted as H_{inf}) is expressed in terms of the slow-roll parameter ϵ as

$$H_{\text{inf}} \simeq \sqrt{\epsilon} \times 10^{15} \text{ GeV}. \quad (3.5)$$

Thus smaller the ϵ is, lower the energy scale of inflation becomes.

B. Tensor perturbations

The tensor mass term in the action (2.6) gives rise to modifications to the dynamics of the tensor perturbation. Expanding the action (2.6) up to quadratic order in perturbation yields the second-order action of γ_{ij} ,

$$S_T^{(2)} = \frac{M_{\text{pl}}^2}{8} \int d^4x a^3 \delta^{ik} \delta^{jl} \times (\dot{\gamma}_{ij} \dot{\gamma}_{kl} + \gamma_{ij} \nabla^2 \gamma_{kl} - m_g^2 \gamma_{ij} \gamma_{kl}), \quad (3.6)$$

where $\nabla^2 \equiv \delta^{ij} \partial_i \partial_j / a^2$. The resulting equation of motion for γ_{ij} in real space reads

$$\ddot{\gamma}_{ij} + 3H\dot{\gamma}_{ij} - \nabla^2 \gamma_{ij} + m_g^2 \gamma_{ij} = 0. \quad (3.7)$$

We decompose the field γ_{ij} into Fourier modes as

$$\gamma_{ij}(\mathbf{x}, t) = \int \frac{d^3k}{(2\pi)^{3/2}} e^{i\mathbf{k}\cdot\mathbf{x}} \hat{\gamma}_{ij}(\mathbf{k}, t), \quad (3.8)$$

where \mathbf{k} is a comoving wavenumber, and

$$\hat{\gamma}_{ij}(\mathbf{k}, t) = \sum_{s=+, \times} [\gamma(k, t) a_s(\mathbf{k}) + \gamma^*(k, t) a_s^\dagger(-\mathbf{k})] \epsilon_{ij}^{(s)}(\mathbf{k}), \quad (3.9)$$

with $s = +, \times$ being the two polarization states. The polarization tensors $\epsilon_{ij}^{(s)}(\mathbf{k})$, which are transverse and traceless ($k^j \epsilon_{ij}^{(s)} = \delta^{ij} \epsilon_{ij}^{(s)} = 0$), satisfy the normalization $\delta^{ik} \delta^{jl} \epsilon_{ij}^{(s)}(\mathbf{k}) \epsilon_{kl}^{*(s')}(\mathbf{k}) = \delta_{ss'}$. The annihilation and creation operators $a_s(\mathbf{k})$ and $a_s^\dagger(\mathbf{k}')$ obey the commutation relation $[a_s(\mathbf{k}), a_{s'}^\dagger(\mathbf{k}')] = \delta_{ss'} \delta^{(3)}(\mathbf{k} - \mathbf{k}')$. The primordial tensor power spectrum $\mathcal{P}_T(k, t)$ per unit logarithmic frequency interval is given by

$$\mathcal{P}_T(k, t) = 2 \cdot \frac{k^3}{2\pi^2} |\gamma(k, t)|^2, \quad (3.10)$$

where the factor 2 in front comes from the two polarization states.

We introduce a canonically normalized field,

$$v_{ij} \equiv \frac{M_{\text{pl}}}{2} \gamma_{ij}, \quad (3.11)$$

and the corresponding mode functions in the momentum space,

$$v(k, t) \equiv \frac{M_{\text{pl}}}{2} \gamma(k, t). \quad (3.12)$$

Then v obeys the equation of motion,

$$\ddot{v} + 3H\dot{v} + \left(\frac{k^2}{a^2} + m_g^2 \right) v = 0, \quad (3.13)$$

or in terms of the conformal time $\tau = \int^t dt/a$,

$$v'' + 2\mathcal{H}v' + (k^2 + m_g^2 a^2) v = 0, \quad (3.14)$$

where a prime represents the derivative with respect to conformal time, $' = \partial/\partial\tau$ and $\mathcal{H} = a'/a$. It satisfies the Klein-Gordon normalization,

$$v v^{*'} - v' v^* = \frac{i}{a^2}. \quad (3.15)$$

The mode function that satisfies the above is called a positive frequency function.

C. Tensor power spectrum for $m_g^2/H^2 \ll 1$

Assuming that $m_g^2 \ll H^2$ and $|\dot{m}_g/(Hm_g)| \ll 1$ during inflation and adopting the de Sitter background approximation, $a \simeq (-H\tau)^{-1}$, which is valid as long as the wavelength is shorter than the Hubble radius, $k/a \gtrsim H$ ($\leftrightarrow k \gtrsim \mathcal{H}$), the natural positive frequency function in the limit $k \gg \mathcal{H}$ is given by

$$v = \frac{1}{\sqrt{2(k/a)a^3}} e^{-i \int^t dt k/a} = \frac{1}{a\sqrt{2k}} e^{-ik\tau}. \quad (3.16)$$

This solution is valid as long as $k/\mathcal{H} \approx (-k\tau) \gtrsim 1$, and coincides with the mode function of the Bunch-Davies vacuum in the pure de Sitter limit.

As the Universe expands and the comoving wavelength becomes greater than the Hubble radius, $k/\mathcal{H} \approx (-k\tau) \lesssim 1$, the de Sitter approximation is no longer valid. In this case, on the other hand, the perturbation v ceases its oscillations and the solution is given by the friction-dominated slow-roll solution,

$$v \simeq C \exp \left[- \int^t \frac{m_g^2}{3H} dt \right]. \quad (3.17)$$

The constant C is determined by matching the two solutions (3.16) and (3.17) at the horizon crossing time t_k characterized by $k = a(t_k)H(t_k)$ ($\leftrightarrow k/\mathcal{H}(\tau_k) \approx -k\tau_k = 1$). This leads to the solution for $t > t_k$,

$$v(k, t) = \frac{H(t_k)}{\sqrt{2k^3}} \exp \left[- \int_{t_k}^t \frac{m_g^2}{3H} dt \right], \quad (3.18)$$

apart from an irrelevant phase factor.

The tensor power spectrum (3.10) is then given by

$$\mathcal{P}_T(k, t) = \frac{2k^2}{\pi^2 M_{\text{pl}}^2 a^2}, \quad \text{for } k \gg aH, \quad (3.19)$$

and

$$\mathcal{P}_T(k, t) = \frac{2H^2(t_k)}{\pi^2 M_{\text{pl}}^2} \exp \left[- \int_{t_k}^t \frac{2m_g^2}{3H} dt \right], \quad \text{for } k \ll aH. \quad (3.20)$$

If m_g^2/H^2 remains small until the end of inflation, say until $t = t_f$, and its effect could be neglected after inflation, the spectrum for the modes $k \ll aH$ becomes

$$\mathcal{P}_T(k, t_f) = \frac{2H^2(N_k)}{\pi^2 M_{\text{pl}}^2} \exp \left[- \int_0^{N_k} \frac{2m_g^2}{3H^2} dN \right], \quad (3.21)$$

where $dN = -Hdt$, and N_k is the number of e-folding at Hubble horizon crossing counted backward from the end of inflation, $N_k = \int_{t_k}^{t_f} H dt$. The spectrum index is given by

$$n_T \equiv \frac{d \ln \mathcal{P}_T}{d \ln k} = -2\epsilon(t_k) + \frac{2m_g^2}{3H^2}(t_k). \quad (3.22)$$

The tensor-to-scalar ratio reads

$$r = 16\epsilon(t_k) \exp \left[- \int_0^{N_k} \frac{2m_g^2}{3H^2} dN \right]. \quad (3.23)$$

Thus the blue-tilted spectrum may be realized if $m_g^2/H^2 > 3\epsilon$ at the time of Hubble horizon crossing. However, due to the evolution of the massive tensor on super-horizon scales, the tensor-to-scalar ratio at CMB observation scales, $N_k \gg 1$, would be substantially suppressed in comparison with the massless tensor case.

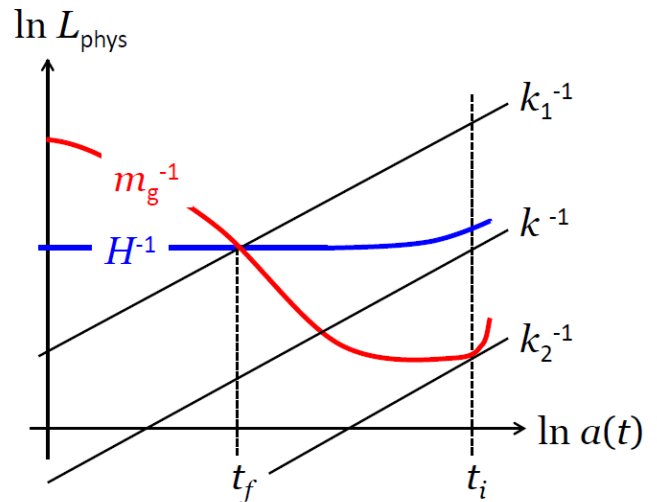


FIG. 1. The physical scales of our interest at which the tensor power spectrum changes its shape are depicted in the space-time diagram. At $t > t_f$ the amplitude of the tensor modes $v(k, t)$ outside the Hubble horizon is nearly constant in time, while the modes inside the Hubble horizon behave as $\propto a^{-1}$. At $t_f < t < t_i$, the modes at $a/k > m_g^{-1}$ evolve as $a^{-3/2}$, while those at $a/k < m_g^{-1}$ behave as a^{-1} .

D. Tensor spectrum after the transition from $m_g^2 \ll H^2$ to $m_g^2 \gg H^2$ during inflation

If the tensor mass is too heavy ($m_g^2/H^2 \gg 1$) during inflation, the tensor perturbation is subject to strong suppression. To avoid such suppression, we need $m_g^2/H^2 \ll 1$ during the most stage of inflation. For the broad parametric resonance to occur right after inflation, on the other hand, the ratio m_g^2/H^2 must be larger than unity at the onset of reheating. Thus, we consider the case where the transition from the almost massless regime $m_g^2/H^2 \ll 1$ to the massive regime $m_g^2/H^2 \gg 1$ occurs at the late stage of inflation, and solve the evolution of the mode functions until the onset of inflaton oscillations.

In the following, we assume that the tensor mass satisfies $m_g^2 \ll H^2$ initially, gradually grows and crosses $m_g^2 \simeq H^2$ at $t = t_f$, and becomes $m_g^2 \gg H^2$ until $t = t_i$ ($> t_f$), where t_i is the time at the onset of the oscillatory stage of ϕ . For the sake of analytical estimates, we employ the approximation that $m_g^2 \ll H^2$ at $t < t_f$, $m_g^2 = H^2$ at $t = t_f$, and $m_g^2 \gg H^2$ at $t_f < t < t_i$, which is qualitatively valid for most of the modes of interest. For reference, the physical scales of our interest are depicted in Fig. 1.

First, let us consider the modes $k < m_g(t_f)a(t_f) = H(t_f)a(t_f) \equiv k_1$. For these modes, since $k/a \ll H \ll m_g$

for $t > t_f$, Eq. (3.13) may be easily solved to give

$$v(k, t) = v(k, t_f) \left[\frac{a(t_f)}{a(t)} \right]^{3/2} \left[\frac{m_g(t_f)}{m_g(t)} \right]^{1/2} e^{\pm i \int^t m_g dt}, \quad (3.24)$$

where $e^{\pm i \int^t m_g dt}$ is an abbreviation for $\alpha e^{-i \int^t m_g dt} + \beta e^{+i \int^t m_g dt}$ with $|\alpha|^2 + |\beta|^2 = 1$. We adopt the above notation since the explicit values of α and β are unnecessary for our discussion. The value of $v(k, t_f)$ is given by Eq. (3.18) with $t = t_f$. Taking into account the variation of H from $t = t_k$ ($\leftrightarrow N = N_k$) to $t = t_f$ ($\leftrightarrow N = N_f$), it follows that $H(t_k) = H(t_f) \exp(\int_{N_f}^{N_k} \epsilon dN)$. Then, we obtain

$$v(k, t_f) = \frac{H(t_f)}{\sqrt{2k^3}} \exp \left[\int_{N_f}^{N_k} \left(\epsilon - \frac{m_g^2}{3H^2} \right) dN \right]. \quad (3.25)$$

The resulting power spectrum at the end of inflation is given by

$$\mathcal{P}_T(k, t_i) = \mathcal{P}_T(k_1, t_i) \exp \left[2 \int_{N_f}^{N_k} \left(\epsilon - \frac{m_g^2}{3H^2} \right) dN \right], \quad (3.26)$$

for $k < k_1$,

where

$$\mathcal{P}_T(k_1, t_i) = \frac{2H^2(t_f) m_g(t_f)}{\pi^2 M_{\text{pl}}^2 m_g(t_i)} e^{-3N_{f \rightarrow i}}, \quad (3.27)$$

and $N_{f \rightarrow i} \equiv \ln[a(t_i)/a(t_f)]$. Note that $H(t_f) = m_g(t_f)$ by definition.

Let us now turn to the modes in the range $k_1 < k < k_2$ where $k_2 \equiv m_g(t_i)a(t_i)$. The highest wavenumber is set at $k = k_2$ because the effect of the mass term would be negligible for the modes with $k > k_2$ at any stage of the Universe. For the modes $k_1 < k < k_2$ the frequency $\omega_k \equiv \sqrt{k^2/a^2 + m_g^2}$ is much larger than H by the end of inflation, so the solution to Eq. (3.13) yields

$$v(k, t) = \frac{1}{a^{3/2} \sqrt{2\omega_k}} e^{\pm i \int^t \omega_k dt}. \quad (3.28)$$

The perturbation in the range $k_1 < k < k_2$ crosses $k = m_g a$ at an epoch, say $t = t_m$, where t_m is in the range $t_f < t_m < t_i$. For $t < t_m$ we have $k^2/a^2 \gg m_g^2$, so Eq. (3.28) reproduces the early-time vacuum solution (3.16) with $|v(k, t)| \propto a^{-1}$. For $t > t_m$ we have $\omega_k \simeq m_g$ and hence $|v(k, t)| \propto a^{-3/2}$ from Eq. (3.28). The resulting amplitude at the end of inflation is given by

$$|v(k, t_i)| = \frac{1}{a(t_i)^{3/2} \sqrt{2m_g(t_i)}}, \quad (3.29)$$

which leads to the highly blue-tilted spectrum

$$\mathcal{P}_T(k, t_i) = \mathcal{P}_T(k_1, t_i) \left(\frac{k}{k_1} \right)^3, \quad \text{for } k_1 < k < k_2. \quad (3.30)$$

For the modes $k > k_2$ the solution to Eq. (3.13) is given by Eq. (3.28) with $\omega_k \simeq k/a$, so that the perturbation evolves as $|v(k, t)| \propto a^{-1}$. The power spectrum at the end of inflation has the scale-dependence

$$\begin{aligned} \mathcal{P}_T(k, t_i) &= \frac{2}{\pi^2 M_{\text{pl}}^2} \left(\frac{k}{a(t_i)} \right)^2 \\ &= \mathcal{P}_T(k_2, t_i) \left(\frac{k}{k_2} \right)^2, \quad \text{for } k > k_2, \end{aligned} \quad (3.31)$$

which is smoothly matched with Eq. (3.30) at $k = k_2 = m_g(t_i)a(t_i)$, where

$$\mathcal{P}_T(k_2, t_i) = \mathcal{P}_T(k_1, t_i) \left(\frac{k_2}{k_1} \right)^3 = \frac{2m_g^2(t_i)}{\pi^2 M_{\text{pl}}^2}. \quad (3.32)$$

In summary, the power spectrum at the end of inflation is given by Eq. (3.26) for $k < k_1$, Eq. (3.30) for $k_1 < k < k_2$, and Eq. (3.31) for $k > k_2$. As clear from the above discussion, the spectrum suffers from strong suppression if the transition from the almost massless stage to the massive stage takes too many e-foldings. In Sec. V, we will confirm the above analytic estimation in the Starobinsky model by using the tensor mass squared (2.12).

IV. PARAMETRIC RESONANCE OF GRAVITATIONAL WAVES DURING REHEATING

The inflationary epoch is followed by the reheating stage in which the inflaton field oscillates around its potential minimum. If the potential has a minimum at $\phi = 0$, it can be expanded in the following form

$$V(\phi) = \frac{1}{2} M^2 \phi^2 + \dots, \quad (4.1)$$

where M is the inflaton mass during reheating and the dots stand for corrections to the leading-order term $M^2 \phi^2/2$.

The end of inflation depends on the form of the potential $V(\phi)$ in the preceding inflationary epoch. In chaotic inflation where the potential is exactly given by $V(\phi) = M^2 \phi^2/2$ [31], the field value at the end of inflation can be estimated as $\phi_{\text{end}} = \sqrt{2} M_{\text{pl}}$ from the condition $\epsilon_V = 1$. In this case, the mass scale M is of the same order as the Hubble parameter H_i at the onset of reheating.

If we consider the potential $V(\phi) = V_0(1 - e^{-\alpha\phi/M_{\text{pl}}})^2$ of the so-called α -attractor model [32], the leading-order contribution to $V(\phi)$ around $\phi = 0$ is given by Eq. (4.1) with $M^2 = 2V_0\alpha^2/M_{\text{pl}}^2$. The slow-roll parameter for this potential is $\epsilon_V = 2\alpha^2(e^{\alpha\phi/M_{\text{pl}}} - 1)^{-2}$, so ϕ_{end} tends to be smaller for larger α . The Starobinsky model discussed later in Sec. V corresponds to $\alpha = \sqrt{6}/3$, in which case $\phi_{\text{end}} = 0.94M_{\text{pl}}$. If $\alpha = 100$, then $\phi_{\text{end}} = 0.05M_{\text{pl}}$. For

$\phi_{\text{end}} \ll M_{\text{pl}}$, it follows that $H_i \ll M$. As we will see below, for smaller ϕ_{end} , the broad parametric resonance after inflation tends to be less efficient.

During reheating, the inflaton energy density finally decays to the radiation energy density ρ_r . We consider the Born decay with the friction term $\Gamma\dot{\phi}$ in the inflaton equation of motion, where Γ is a decay constant [33, 34]. On the FLRW background the dynamical equations of motion are then given by

$$3M_{\text{pl}}^2 H^2 = \frac{1}{2}\dot{\phi}^2 + V(\phi) + \rho_r, \quad (4.2)$$

$$\ddot{\phi} + (3H + \Gamma)\dot{\phi} + V_{,\phi} = 0, \quad (4.3)$$

$$\dot{\rho}_r + 4H\rho_r = \Gamma\dot{\phi}^2. \quad (4.4)$$

The period driven by oscillations of the massive inflaton is characterized by the transient matter era in which the scale factor evolves as $a \propto t^{2/3}$. At the early stage of reheating, where the condition $H \gg \Gamma$ is satisfied, the radiation is not yet sufficiently generated, so Eqs. (4.2) and (4.3) reduce, respectively, to $4M_{\text{pl}}^2/(3t^2) \simeq \dot{\phi}^2/2 + M^2\phi^2/2$ and $\ddot{\phi} + (2/t)\dot{\phi} + M^2\phi \simeq 0$. The solution to ϕ compatible with these equations is given by

$$\phi(t) \simeq \sqrt{\frac{8}{3}} \frac{M_{\text{pl}}}{Mt} \sin(Mt + \theta_0), \quad (4.5)$$

where θ_0 is an arbitrary constant. For the inflationary models in which ϕ_{end} is of the order M_{pl} (like chaotic inflation and Starobinsky model), the initial time t_i at the onset of reheating corresponds to $t_i = \mathcal{O}(1/M)$. For the models with $\phi_{\text{end}} \ll M_{\text{pl}}$ (like the α -attractor with $\alpha \gg 1$), we have that $Mt_i \gg 1$.

After the Hubble expansion rate H drops below Γ , the solution to Eq. (4.3) changes to

$$\phi(t) \propto e^{-\Gamma(t-t_i)/2} \sin(Mt + \theta_0), \quad (4.6)$$

where we used the condition $\Gamma \ll M$. Hence the field ϕ starts to decay rapidly to generate the radiation around the time defined by $t_\Gamma \equiv 1/\Gamma$. The reheating temperature is estimated as [25, 35]

$$T_\Gamma = 1.1g_*^{-1/4} \sqrt{\Gamma M_{\text{pl}}}, \quad (4.7)$$

where g_* is the relativistic degrees of freedom at t_Γ .

For concreteness, let us first consider the ϕ -dependent tensor mass squared given by Eq. (2.12) with $b = \mathcal{O}(1)$ and $n = \mathcal{O}(1)$. For the models with $\phi_{\text{end}} \lesssim M_{\text{pl}}$ we have $b(\phi_{\text{end}}/M_{\text{pl}})^n \lesssim 1$, so $m_g^2(\phi)$ can be approximated as $\lambda\phi^2$. Then, the coherent oscillation of inflaton leads to the excitation of the perturbation v by the parametric resonance. Introducing the rescaled field $X_T = a^{3/2}v$ in Eq. (3.13), it follows that

$$\ddot{X}_T + \left[\frac{k^2}{a^2} + \lambda\phi^2 e^{-b(\phi/M_{\text{pl}})^n} - \frac{9}{4}H^2 - \frac{3}{2}\dot{H} \right] X_T = 0. \quad (4.8)$$

On using the solution (4.5) with $\theta_0 = 0$, we can express Eq. (4.8) in form of the Mathieu equation

$$\frac{d^2 X_T}{dz^2} + [A_k - 2q \cos(2z)] X_T = 0, \quad (4.9)$$

where

$$A_k = \frac{k^2}{M^2 a^2} + 2q - \frac{9H^2}{4M^2} - \frac{3\dot{H}}{2M^2}, \quad (4.10)$$

$$q = \frac{2\lambda}{3} \left(\frac{M_{\text{pl}}}{M} \right)^2 \frac{e^{-b(\phi/M_{\text{pl}})^n}}{z^2}, \quad (4.11)$$

$$z = Mt. \quad (4.12)$$

The broad parametric resonance occurs in the regime where the parameter q is much larger than 1 [24, 25]. Since the Hubble parameter during reheating can be estimated as $H^2 \simeq M^2\phi^2/(3M_{\text{pl}}^2)$, it follows that $m_g^2/H^2 \simeq 3\lambda(M_{\text{pl}}/M)^2 e^{-b(\phi/M_{\text{pl}})^n}$. For the models in which ϕ_{end} is of the order M_{pl} , we have $z_i = Mt_i = \mathcal{O}(1)$ and hence the resonance parameter q is of the similar order to m_g^2/H^2 at the onset of reheating ($t = t_i$). In such cases, as long as the condition

$$\lambda \left(\frac{M_{\text{pl}}}{M} \right)^2 \gg 1 \quad (4.13)$$

is satisfied, both q and m_g^2/H^2 are much larger than 1 at $t = t_i$. Since q decreases in proportion to t^{-2} , the perturbation X_T crosses many instability and stability bands present for the system of the Mathieu equation (4.9) [25, 36]. Even if the resonance occurs stochastically in the expanding Universe, the rapid movement of inflaton around $\phi = 0$ leads to the non-adiabatic growth of tensor perturbations.

For the models with $\phi_{\text{end}} \ll M_{\text{pl}}$ we have $z_i = Mt_i \gg 1$, so the parameter q is much smaller than the ratio m_g^2/H^2 at $t = t_i$. This means that, even if m_g^2 grows to a value much larger than H^2 at the end of inflation, the parametric resonance tends to be less efficient relative to the case $\phi_{\text{end}} = \mathcal{O}(M_{\text{pl}})$. In such cases, we need to choose a larger coupling constant λ for the realization of the excitation of GWs similar to that for $\phi_{\text{end}} = \mathcal{O}(M_{\text{pl}})$.

During the coherent oscillation of inflaton the term $k^2/(M^2 a^2)$ is in proportion to $t^{-4/3}$, which decreases more slowly relative to the term $2q$. If the condition $k^2/(M^2 a_i^2) > 2q_i$ is satisfied at the beginning of reheating (where the subscript “ i ” represents quantities at $t = t_i$), the gradient term $k^2/(M^2 a^2)$ dominates over the other terms in the square bracket of Eq. (4.9) and hence the broad parametric resonance does not occur. Then, we obtain the cut-off wavenumber

$$\frac{k_{\text{cut}}}{a_i H_i} = \sqrt{\frac{4\lambda}{3}} \frac{M_{\text{pl}}}{H_i} \frac{e^{-b(\phi_i/M_{\text{pl}})^n/2}}{z_i}. \quad (4.14)$$

The GWs with wavenumbers in the range

$$k \lesssim k_{\text{cut}}, \quad (4.15)$$

are subject to the parametric amplification during reheating. Since $e^{-b(\phi_i/M_{\text{pl}})^n/2}$ is of the order unity for $\phi_i \lesssim M_{\text{pl}}$, we have $k_{\text{cut}}/(a_i H_i) \approx \sqrt{\lambda}(M_{\text{pl}}/H_i)z_i^{-1}$.

The broad parametric resonance ends after q drops below the order of 1. The narrow parametric resonance occurs in the instability bands ranging in the region $0.3 \lesssim q \lesssim 0.8$ [25]. The end of amplification (labelled by the subscript ‘‘e’’) is characterized by the condition $q_e \simeq 0.3$, such that

$$z_e \simeq 1.5\sqrt{\lambda}\frac{M_{\text{pl}}}{M}. \quad (4.16)$$

The typical wavenumber k_* associated with the parametric excitation of GWs corresponds to the mode $k_*^2/(M^2 a_e^2) \simeq 2q_e \simeq 0.6$, i.e.,

$$\frac{k_*}{a_i H_i} \simeq 0.8\frac{M}{H_i}\left(\frac{z_e}{z_i}\right)^{3/2}. \quad (4.17)$$

For the modes $k > k_*$, the gradient term $k^2/(M^2 a^2)$ starts to dominate over the resonance term $2q \cos(2z)$ before the end of amplification, so the parametric resonance tends to be less efficient. On the other hand, the resonance does not occur for the modes $k > k_{\text{cut}}$. If $\lambda \simeq 10^{-6}$, $M \simeq 10^{-5}M_{\text{pl}}$, $H_i \simeq 0.5M$, and $z_i = 1$, for example, we have $k_*/(a_i H_i) \simeq 45$ and $k_{\text{cut}}/(a_i H_i) \simeq 200$ with $z_e \simeq 150$.

We also consider the $\dot{\phi}$ -dependent tensor mass squared given by Eq. (2.13). Employing the background solution (4.5) with $\theta_0 = \pi/2$, the rescaled field $X_T = a^{3/2}v$ obeys the Mathieu equation (4.9) with

$$q = \frac{2\mu}{3z^2}, \quad (4.18)$$

where A_k and z are defined in the same as Eqs. (4.10) and (4.12), respectively. Compared to Eq. (4.11), there is the correspondence $\mu \rightarrow \lambda(M_{\text{pl}}/M)^2$ and $e^{-b(\phi/M_{\text{pl}})^n} \rightarrow 1$. For the models with $\phi_{\text{end}} = \mathcal{O}(M_{\text{pl}})$, i.e., $z_i = Mt_i = \mathcal{O}(1)$, the broad parametric resonance occurs for

$$\mu \gg 1. \quad (4.19)$$

For the models with $\phi_{\text{end}} \ll \mathcal{O}(M_{\text{pl}})$ we have $z_i \gg \mathcal{O}(1)$, so the broad resonance is less efficient relative to the case $\phi_{\text{end}} = \mathcal{O}(M_{\text{pl}})$ for the same coupling μ .

The discussion given between Eq. (4.14) and (4.17) is valid by replacing λ with $\mu(M/M_{\text{pl}})^2$, e.g., $k_{\text{cut}}/(a_i H_i) = \sqrt{4\mu/3}(M/H_i)z_i^{-1}$ and $z_e \simeq 1.5\sqrt{\mu}$.

V. STAROBINSKY INFLATION WITH THE ϕ -DEPENDENT TENSOR MASS

For the tensor mass squared given by Eq. (2.12), we numerically compute the primordial tensor power spectrum at the end of reheating for the inflaton potential

$$V(\phi) = \frac{3}{4}M^2 M_{\text{pl}}^2 \left[1 - e^{-\sqrt{6}\phi/(3M_{\text{pl}})}\right]^2. \quad (5.1)$$

This follows from the Lagrangian $f(R) = R + R^2/(6M^2)$ after a conformal transformation to the Einstein frame [12]. The scalar degree of freedom ϕ is related to the Ricci scalar R , as $\phi = \sqrt{3/2}M_{\text{pl}} \ln[1 + R/(3M^2)]$. Expanding the potential (5.1) around $\phi = 0$, the leading-order contribution corresponds to $M^2 \phi^2/2$.

For the potential (5.1), the slow-roll parameter (2.11) is given by

$$\epsilon_V = \frac{4}{3} \left[e^{\sqrt{6}\phi/(3M_{\text{pl}})} - 1 \right]^{-2}, \quad (5.2)$$

so that the end of inflation ($\epsilon_V = 1$) corresponds to the field value $\phi_{\text{end}} = 0.94M_{\text{pl}}$. The inflationary expansion is realized in the regime $\phi \gtrsim M_{\text{pl}}$. The e-folding number associated with the field value ϕ during inflation can be estimated as

$$N = \frac{1}{M_{\text{pl}}^2} \int_{\phi_{\text{end}}}^{\phi} \frac{V}{V_{,\tilde{\phi}}} d\tilde{\phi} \simeq \frac{3}{4} e^{\sqrt{6}\phi/(3M_{\text{pl}})} - \frac{\sqrt{6}\phi}{4M_{\text{pl}}}, \quad (5.3)$$

where we neglected the contribution arising from ϕ_{end} . Taking the dominant contributions in Eqs. (5.2) and (5.3), we obtain the following relation

$$\epsilon \simeq \frac{3}{4N^2}. \quad (5.4)$$

For $N = 55$, we have $\epsilon \simeq 2.5 \times 10^{-4}$, so the Hubble parameter in Starobinsky inflation corresponds to $H_{\text{inf}} \simeq 10^{13}$ GeV from Eq. (3.5). The other slow-roll parameter (3.4) is approximately given by $\eta_V \simeq -(4/3)e^{-\sqrt{6}\phi/(3M_{\text{pl}})} \simeq -1/N$, so the scalar spectral index (3.3) reads

$$n_s - 1 \simeq -\frac{2}{N}, \quad (5.5)$$

which is $n_s = 0.964$ for $N = 55$. This value is within the 1σ observational contour constrained by the Planck CMB data [6].

For the massless tensor ($m_g = 0$), the power spectrum at the end of inflation is given by Eq. (3.21), i.e., $\mathcal{P}_T \simeq 2H^2/(\pi^2 M_{\text{pl}}^2)$ with

$$n_t \simeq -\frac{3}{2N^2}, \quad r \simeq \frac{12}{N^2}. \quad (5.6)$$

For $N = 55$ the tensor-to-scalar ratio is $r \simeq 4.0 \times 10^{-3}$, which is much below the current CMB bound ($r < 0.11$) [6].

For the massive tensor, the existence of the parametric resonance offers the possibility of amplifying tensor perturbations to the detectable level in CMB measurements. In the following, we will numerically compute the primordial tensor power spectra both at the onset and the end of amplification. Since ϕ_{end} is of order M_{pl} , we identify the onset of reheating as $t_i = 1/M$.

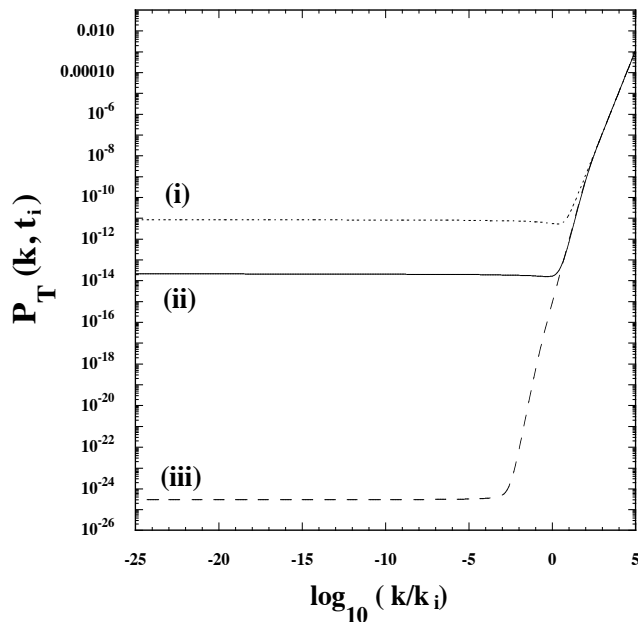


FIG. 2. The primordial tensor power spectra at the onset of reheating ($t = t_i$) for the potential (5.1) with $M = 1.3 \times 10^{-5} M_{\text{pl}}$. Each curve corresponds to (i) the massless tensor ($m_g^2 = 0$), (ii) the tensor mass squared (2.12) with $n = 2$, $b = 4$, $\lambda = 5 \times 10^{-7}$, and (iii) the tensor mass squared (2.12) with $n = 1$, $b = 4$, $\lambda = 5 \times 10^{-7}$. The suppression of GWs induced by the heavy tensor mass during inflation tends to be less significant for larger values of n and b .

A. Tensor power spectrum at the onset of reheating

We start to integrate the tensor perturbation Eq. (3.14) from the $N = 64$ e-folding before the end of inflation. The initial condition for the mode functions deep inside the Hubble horizon is given by Eq (3.16). In Fig. 2, we show the primordial tensor power spectrum just after the end of inflation for three different tensor masses.

For the standard massless tensor, which corresponds to the case (i) in Fig. 2, the power spectrum of GWs which crossed the Hubble horizon before the end of inflation ($k \lesssim k_i \equiv a_i H_i$) is given by $\mathcal{P}_T \simeq 2H^2/(\pi^2 M_{\text{pl}}^2)$, while, for $k \gtrsim k_i$, it is given by the spectrum (3.31) with the scale-dependence $\mathcal{P}_T \propto k^2$.

The plot (ii) in Fig. 2 is the tensor power spectrum at $t = t_i$ for the tensor mass squared (2.12) with $n = 2$, $b = 4$, and $\lambda = 5 \times 10^{-7}$. In this case, the tensor mass is in the regime $m_g^2 \lesssim H^2$ during most of the inflationary epoch. The transition to the regime $m_g^2 \gtrsim H^2$ rapidly occurs just before the end of inflation (with the e-folding number $N_{f \rightarrow i} = 0.7$), so the suppression factor $\exp(-3N_{f \rightarrow i})$ in Eq. (3.26) is of order 0.1. In this case, the wavenumber k_1 discussed in Sec. III D corresponds to $k_1 \simeq e^{-N_{f \rightarrow i}} k_i \simeq 0.5k_i$. For the modes

$k \ll k_1$, the numerically derived power spectrum is nearly scale-invariant, whose property is consistent with the analytic result (3.26). As estimated from Eq. (3.30), the power spectrum has the dependence $\mathcal{P}_T \propto k^3$ for $k_1 \ll k \lesssim k_2 \simeq 10^{5/2} k_i$. In the numerical simulation of Fig. 2, there is an intermediate regime around $0.5k_i < k < 5k_i$ in which the power spectrum has the scale-dependence $\mathcal{P}_T \propto k^n$ with $0 < n < 3$. The highly blue-tilted spectrum $\mathcal{P}_T \propto k^3$ arises for $k \gtrsim 5k_i$. For the modes $k \gtrsim k_2 \simeq 10^{5/2} k_i$, the scale dependence changes to $\mathcal{P}_T \propto k^2$ according to Eq. (3.31).

In the case (iii) of Fig. 2, the power n in the tensor mass is smaller than that in the case (ii), so the period of the regime $m_g^2 \gtrsim H^2$ during inflation is longer. Hence the perturbations with the wavenumber $k \lesssim 10^{-5/2} k_i$ are subject to stronger suppression. In this case, the power spectrum is given by Eq. (3.30) for the modes $10^{-5/2} k_i \lesssim k \lesssim 10^{5/2} k_i$ and by Eq. (3.31) for the modes $k \gtrsim 10^{5/2} k_i$.

These results show that the suppression of \mathcal{P}_T tends to be smaller for $m_g^2(\phi)$ undergoing a faster transition from the region $m_g^2 \lesssim H^2$ to the region $m_g^2 \gtrsim H^2$. This corresponds to the choice of larger values of n and b in Eq. (2.12).

B. Tensor power spectrum after inflaton decay

During reheating, the tensor perturbation is subject to the broad parametric amplification for the coupling constant λ satisfying the condition (4.13). For concreteness of our discussion, in this subsection we consider the model parameters $\lambda = 4.8 \times 10^{-7}$, $M = 1.3 \times 10^{-5} M_{\text{pl}}$, $n = 2$, and $b = 2$. In Fig. 3, we plot the evolution of the power spectrum \mathcal{P}_T for these model parameters.

The mode which crossed the Hubble horizon at $N = 55$ e-folding before the end of inflation corresponds to the perturbation associated with the observation of CMB temperature anisotropies. As we see in Fig. 3, this large-scale tensor mode is temporarily nearly frozen after horizon crossing ($k < aH$) and then it starts to decrease when the tensor mass squared becomes comparable to H^2 during inflation. In spite of the decrease of \mathcal{P}_T by a factor of $\mathcal{O}(10^{-6})$ by the end of inflation, the parametric amplification of GWs during reheating enhances \mathcal{P}_T by a factor of $\mathcal{O}(10^8)$, resulting in the final enhancement factor of $\mathcal{O}(10^2)$. For larger λ , the peak value of \mathcal{P}_T after the amplification ($q \simeq 0.3$) generally increases.

In Fig. 3, we also show the evolution of \mathcal{P}_T for the mode which crossed the Hubble horizon at the $N = 16$ e-folding before the end of inflation. The evolution of \mathcal{P}_T during inflation and reheating is similar to that for the mode with $N = 55$.

The modes that crossed the Hubble radius a few e-folding ($N \lesssim 5$) before the end of inflation, namely those in the range $k_1 < k < k_i$, exhibit different evolutionary behavior to the larger-scale modes. They are not subject to the strong suppression during inflation as discussed in Sec. III D. Then, the peak values of \mathcal{P}_T reached for these

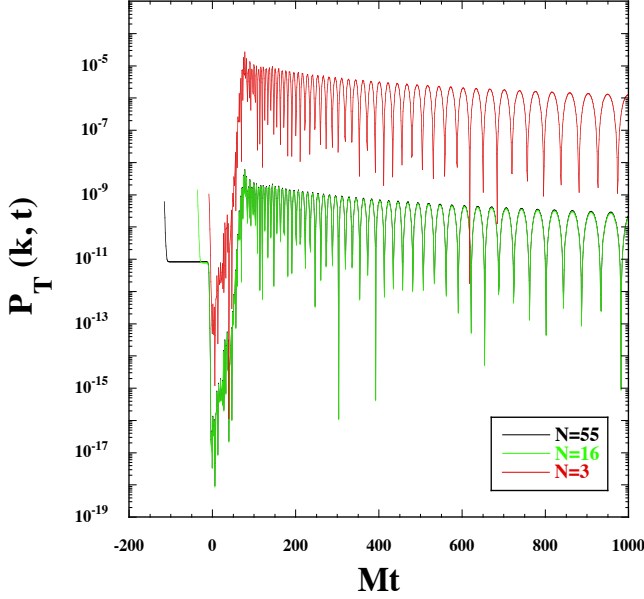


FIG. 3. Evolution of the tensor power spectrum in Starobinsky inflation with $M = 1.3 \times 10^{-5} M_{\text{pl}}$ for the tensor mass squared (2.12) with $\lambda = 4.8 \times 10^{-7}$, $n = 2$, and $b = 2$. The three curves correspond to the modes which crossed the Hubble radius at $N = 55, 16, 3$ e-folding before the end of inflation, respectively.

small-scale perturbations are larger than those for the modes which crossed the Hubble horizon earlier ($N \gtrsim 5$), see Fig. 3 for $N = 3$. Numerically, we also studied the evolution of GWs for smaller-scale modes ($k \gtrsim k_i$) and confirmed that the parametric resonance occurs for the wavenumber $k < k_{\text{cut}} = \mathcal{O}(10^2 k_i)$.

In Fig. 3, we find that the power spectra \mathcal{P}_T start to decrease after reaching their peak values. This comes from the fact that the inflaton coherently oscillates according to Eq. (4.5) up to the time $t_{\Gamma} \simeq 1/\Gamma$. For $t_i < t < t_{\Gamma}$, we take the time average of the tensor mass squared over oscillations, such that $\langle m_g^2(\phi) \rangle \simeq \langle \lambda \phi^2 \rangle \simeq 4\lambda M_{\text{pl}}^2 / (3M^2 t^2)$. Provided that $\langle m_g^2(\phi) \rangle$ dominates over the gradient term k^2/a^2 , Eq. (3.13) reduces to

$$\ddot{v} + \frac{2}{t}\dot{v} + \frac{4\lambda M_{\text{pl}}^2}{3M^2 t^2}v \simeq 0, \quad (5.7)$$

where we used the fact that the scale factor evolves as $a \propto t^{2/3}$ for $t_i < t < t_{\Gamma}$. The solution to this equation is given by

$$v \propto t^{-1/2 \pm i\Omega}, \quad (5.8)$$

where $\Omega = (48\lambda M_{\text{pl}}^2/M^2 - 9)^{1/2}/6 > 0$ under the condition (4.13), i.e., $\lambda M_{\text{pl}}^2/M^2 \gg 1$. So the amplitude of GWs decreases as $|v| \propto t^{-1/2}$. Thus, for large-scale modes satisfying the condition $k^2/a^2 < \langle m_g^2(\phi) \rangle$ until the time t_{Γ} , the amplitude of \mathcal{P}_T decreases as $\langle \mathcal{P}_T \rangle \propto t^{-1}$ after reach-

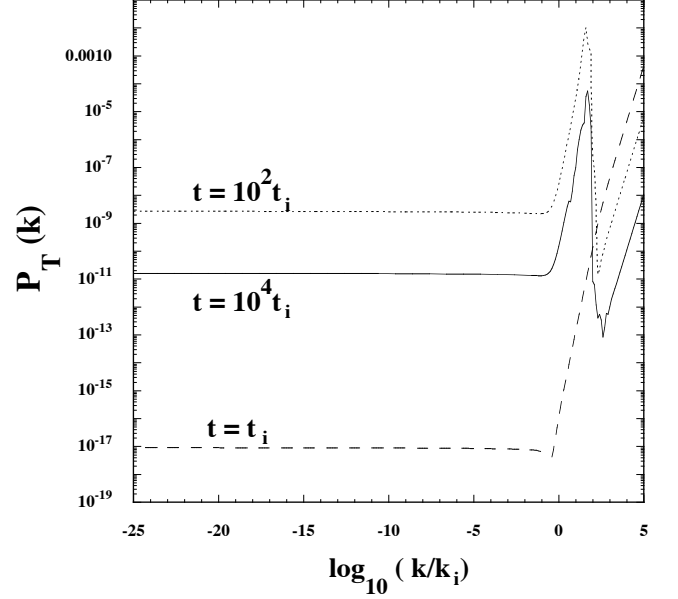


FIG. 4. The tensor power spectra at $t = 10^2 t_i$ and $t = 10^4 t_i$ for the potential (5.1) with $M = 1.3 \times 10^{-5} M_{\text{pl}}$ in the presence of the tensor mass squared (2.12) with $\lambda = 4.8 \times 10^{-7}$, $n = 2$, and $b = 2$. We also show the spectrum at the onset of reheating ($t = t_i$). After the amplitude of perturbations reaches the maximum around the time $t \simeq 80 t_i$, it decreases until the moment t_{Γ} at which the inflaton decays to the radiation.

ing its peak value. This behavior is confirmed in the numerical results shown in Fig. 3.

For small-scale modes, it happens that the gradient term k^2/a^2 ($\propto t^{-4/3}$) gets larger than $\langle m_g^2(\phi) \rangle$ ($\propto t^{-2}$) during the time interval $t_i < t < t_{\Gamma}$. The time t_k at which k^2/a^2 becomes equivalent to $\langle m_g^2(\phi) \rangle$ can be estimated as

$$\left(\frac{t_k}{t_i}\right)^{2/3} \simeq 3\lambda \left(\frac{M_{\text{pl}}}{M}\right)^2 \left(\frac{k_i}{k}\right)^2. \quad (5.9)$$

For example, for $M = 1.3 \times 10^{-5} M_{\text{pl}}$ and $\lambda = 4.8 \times 10^{-7}$, we find $t_k \simeq 800 t_i$ for $k = 10 k_i$. During the time interval $t_i < t < t_k$ the amplitude of GWs decreases as $\langle \mathcal{P}_T \rangle \propto t^{-1}$, while, for $t > t_k$, $\langle m_g^2(\phi) \rangle$ gradually becomes negligible relative to the term k^2/a^2 . Provided that $\langle m_g^2(\phi) \rangle \ll k^2/a^2$ the power spectrum evolves as $\langle \mathcal{P}_T \rangle \propto a^{-2} \propto t^{-4/3}$, thus decreasing faster than that during $t_i < t < t_k$.

In Fig. 4, we plot the tensor power spectra at three different epochs ($t = t_i, 10^2 t_i, 10^4 t_i$) for the same model parameters used in Fig. 3. The modes which crossed the Hubble horizon before the onset of reheating are subject to the suppression during inflation, but the parametric resonance leads to the growth of \mathcal{P}_T with a factor of $\mathcal{O}(10^8)$ by the time $t_{\text{max}} \simeq 80 t_i$ (at which \mathcal{P}_T reaches the maximum value). The spectrum of the modes $k \lesssim k_i$ ($\approx 0.3 k_i$) is nearly scale-invariant after the parametric amplification. The GWs with the wavenumber $k_i \lesssim k \lesssim$

$10^2 k_i$ have the highly blue-tiled spectrum (3.30) at the onset of reheating ($t = t_i$). These modes are excited by the parametric resonance, but the perturbations with the wavenumber $k > k_{\text{cut}} \approx 10^2 k_i$ are not subject to the amplification. The power spectrum $\mathcal{P}_T(k)$ at $t = 10^2 t_i$ has a peak around $k \simeq 40 k_i$. For the modes $k \gtrsim 10^2 k_i$, the gradient term k^2/a^2 dominates over $m_g^2(\phi)$, so the power spectrum at $t = 10^2 t_i$ has the dependence $\mathcal{P}_T \propto k^2$.

In summary, during the time interval $t_{\text{max}} < t < t_\Gamma$, the amplitude decreases as $\langle \mathcal{P}_T \rangle \propto t^{-1}$ for the modes $k^2/a^2 \ll \langle m_g^2(\phi) \rangle$, while $\langle \mathcal{P}_T \rangle \propto t^{-4/3}$ for the modes $k^2/a^2 \gg \langle m_g^2(\phi) \rangle$. This behavior can be confirmed by comparing the two spectra at $t = 10^2 t_i$ and $t = 10^4 t_i$ shown in Fig. 4. Depending on the time t_Γ after which ϕ decreases exponentially and hence m_g^2 becomes completely negligible in Eq. (3.13), the amplitude of today's GW power spectrum is different (as we will discuss in Sec. VII). We regard $\mathcal{P}_T(t_\Gamma)$ as the primordial tensor power spectrum at which the super-horizon tensor perturbations ($k/a < H$) are frozen. For $t > t_\Gamma$ the GW evolves as a massless field, i.e., $\mathcal{P}_T(t) = \text{constant}$ for $k/a < H$ and $\langle \mathcal{P}_T(t) \rangle \propto a^{-2}$ for $k/a > H$ [37].

The power spectrum $\mathcal{P}_T(t_\Gamma)$ tends to be smaller if we choose smaller values of Γ . If the inflaton decay occurs at the time $10^2 t_i$ in the numerical simulation of Fig. 4, then $\mathcal{P}_T(t_\Gamma)$ is of order 10^{-9} for the modes $k \lesssim k_i$. This case is excluded from the Planck CMB bound $\mathcal{P}_T(t_\Gamma) < 2.4 \times 10^{-10}$ [6]. For $t_\Gamma = 10^4 t_i$ the amplitude of $\mathcal{P}_T(t_\Gamma)$ for large-scale modes is of order 10^{-11} , so this case is consistent with the CMB measurements. For the coupling λ used in Fig. 4, the decay constant is constrained to be $\Gamma \lesssim 10^{-3} M \simeq 10^{-8} M_{\text{pl}}$. It is possible to realize a larger maximum value of \mathcal{P}_T if we choose a larger λ , in which case the upper bound on Γ constrained from CMB tends to be smaller.

The peaks of $\mathcal{P}_T(k)$ appearing in Fig. 4 affect today's energy density spectrum Ω_{GW} of the GW background. In Sec. VII, we will explicitly compute Ω_{GW} for the model discussed above.

VI. LOW-SCALE INFLATION WITH THE ϕ -DEPENDENT TENSOR MASS

In this section, we study the low-scale inflationary scenario in which the slow-roll parameter ϵ is much smaller than 10^{-4} during most stage of inflation. As an explicit example, we consider a very flat potential $V(\phi) \simeq V_0$ for $\phi \gtrsim M_{\text{pl}}$ and then the rapid transition to the potential

$$V(\phi) = \frac{1}{2} M^2 \phi^2, \quad (6.1)$$

occurs around $\phi \approx M_{\text{pl}}$. This type of transition often arises in the context of string inflation [15]. We consider the ϕ -dependent tensor mass squared (2.13) to discuss the dynamics of GWs during inflation and reheating.

We consider the case in which the field value at the end of inflation for the potential (6.1) is determined by the condition $\epsilon_V = 1$, i.e., $\phi_{\text{end}} = \sqrt{2} M_{\text{pl}}$ with $\dot{\phi}_{\text{end}}^2 = (2/3) M^2 M_{\text{pl}}^2$. The Hubble parameter H_i at the onset of reheating ($t = t_i$) obeys the relation $3M_{\text{pl}}^2 H_i^2 = \dot{\phi}_{\text{end}}^2/2 + M^2 \phi_{\text{end}}^2/2$, and hence

$$H_i \simeq \frac{2}{3} M. \quad (6.2)$$

The Hubble parameter H_{inf} related to the observed CMB temperature anisotropies can be regarded as the same order as H_i , so Eq. (3.5) gives the following estimate

$$M \approx \sqrt{\epsilon} \times 10^{15} \text{ GeV}. \quad (6.3)$$

For inflation satisfying the condition $\epsilon \ll 10^{-4}$, the mass scale M is much smaller than 10^{13} GeV with the tensor-to-scalar ratio $r = 16\epsilon \ll 10^{-3}$. For the massless tensor, there is almost no hope for the detection of primordial tensor modes in both CMB and direct detection measurements of GWs, but this is not the case for the massive tensor.

In this section, for concreteness, we adopt the model parameters $\mu = 1.523 \times 10^4$ and $M = 10^8$ GeV, which gives $\phi_{\text{end}} = \mathcal{O}(M_{\text{pl}})$. We note, however, that it is also possible to realize low-scale inflation with $\phi_{\text{end}} \ll M_{\text{pl}}$, in which case $H_i \ll M$. In fact, the potential $V(\phi) = V_0(1 - e^{-\alpha\phi/M_{\text{pl}}})^2$ of the α -attractor model leads to $\phi_{\text{end}} \ll M_{\text{pl}}$ for $\alpha \gg 1$. As we discussed in Sec. IV, however, the broad parametric resonance tends to be less efficient for such smaller values of ϕ_{end} . We need to choose a larger coupling μ to realize the parametric resonance comparable to the case $\phi_{\text{end}} = \mathcal{O}(M_{\text{pl}})$, but in such cases the ratio $m_g^2/H^2 \simeq 2\mu\epsilon$ during inflation gets larger. This leads to the earlier entry to the massive regime $m_g^2 > H^2$, so the GWs are subject to stronger suppression during inflation. Hence we will focus on the low-scale inflation where the transition to the reheating stage given by the potential (6.1) occurs around $\phi \approx M_{\text{pl}}$. In this case, we can identify the time t_i at the onset of reheating as $z_i = Mt_i = 1$.

From Eq. (4.18) the resonance parameter q is much larger than 1 at $t = t_i$ for the coupling $\mu \gg 1$, in which case the broad parametric resonance occurs by the coherent oscillation of the inflaton around $\phi = 0$. In low-scale inflation the slow-roll parameter ϵ during inflation is very much smaller than 1, so even the large coupling with $\mu \gg 1$ allows one to satisfy the condition $m_g^2/H^2 = 2\mu\epsilon \ll 1$. Since ϵ rapidly grows from a tiny value to unity during a very short period around the end of inflation, it is possible to avoid the suppression of GWs induced by the growth of m_g^2 .

We recall that, for the modes $k < k_1$, the tensor power spectrum at the end of inflation is estimated as Eq. (3.26). Since m_g^2/H^2 and ϵ are much smaller than 1 during most stage of low-scale inflation, the power spec-

trum at $t = t_i$ reduces to

$$\begin{aligned} \mathcal{P}_T(t_i) &\simeq \frac{2H_i^2}{\pi^2 M_{\text{pl}}^2} \frac{m_g(t_f)}{m_g(t_i)} e^{-3N_{f \rightarrow i}} \\ &\simeq 3.4 \times 10^{-8} \epsilon_{\text{CMB}} \frac{m_g(t_f)}{m_g(t_i)} e^{-3N_{f \rightarrow i}}, \end{aligned} \quad (6.4)$$

where we have employed the approximations that $H(t_f)$ is equivalent to H_i and that the exponential factor in the second line of Eq. (3.26) equals to 1. Note that ϵ_{CMB} is the slow-roll parameter associated with the perturbation relevant to the CMB observations. There is the suppression factor $e^{-3N_{f \rightarrow i}}$ in Eq. (6.4). As long as inflation ends shortly after m_g^2 crosses H^2 , the suppression induced by the massive tensor is not so significant. For $\epsilon \ll 10^{-4}$ the initial power spectrum (6.4) is much smaller than the order of 10^{-12} , but the oscillating tensor mass makes it possible to amplify the GWs to the detectable level of CMB observations.

The power spectrum at $t = t_i$ for the modes $k_1 < k < k_2$ is given by Eq. (3.30), where k_1 may be expressed as

$$\frac{k_1}{a_i H_i} = \frac{a(t_f)H(t_f)}{a_i H_i} \simeq e^{-N_{f \rightarrow i}}, \quad (6.5)$$

where we used the approximation $H(t_f) \simeq H_i$. For the modes $k > k_1$, we numerically integrate Eq. (3.13) by using the initial condition (3.28) at $t = t_i$. As for the modes $k < k_1$, since they are amplified with the k -independent growth rate from the initial scale-invariant spectrum (6.4), the shape of the spectrum remains the same as the original one, that is, it is almost scale-invariant.

In Fig. 5, we plot the evolution of \mathcal{P}_T from the end of inflation for three different values of k , for the assumed values of the parameters, $\mu = 1.523 \times 10^4$ and $M = 10^8$ GeV. In this case, the suppression factor $e^{-N_{f \rightarrow i}}$ is equal to 0.1, so that the wavenumber (6.5) is given by $k_1/(a_i H_i) = 0.1$, i.e., $k_1 = 0.067M$ by setting $a_i = 1$. In this case, the slow-roll parameter ϵ_{CMB} is of order 10^{-14} from Eq. (3.5) and the tensor mass grows to the value of order $m_g/H_i = \sqrt{2\mu} = \mathcal{O}(10^2)$ by the end of inflation. From Eq. (6.4) we see that the power spectrum for the modes $k < k_1$ is as small as $\mathcal{P}_T(t_i) \approx 10^{-27}$ at the onset of reheating.

As we see in Fig. 5, the power spectrum \mathcal{P}_T for the mode $k = k_1 = 0.067M$ is subject to a strong amplification from the initial value of order 10^{-27} to the maximum value of around 10^{-9} . Analogous to Eq. (4.16) the end of amplification can be estimated as $Mt_e \simeq 1.5\sqrt{\mu} \simeq 180$, which is in good agreement with the numerical results shown in Fig. 5. The power spectrum starts to decrease after reaching its maximum value around $t = t_f$. This is attributed to the fact that the tensor mass squared averaged over oscillations evolves as $\langle m_g^2(\phi^2) \rangle \propto t^{-2}$ up to the time $t_\Gamma = 1/\Gamma$. For the wavenumbers satisfying the condition $k^2/a^2 < \langle m_g^2(\phi^2) \rangle$ until $t = t_\Gamma$, \mathcal{P}_T decreases in proportion to t^{-1} . For $t > t_\Gamma$ the inflaton decays to the

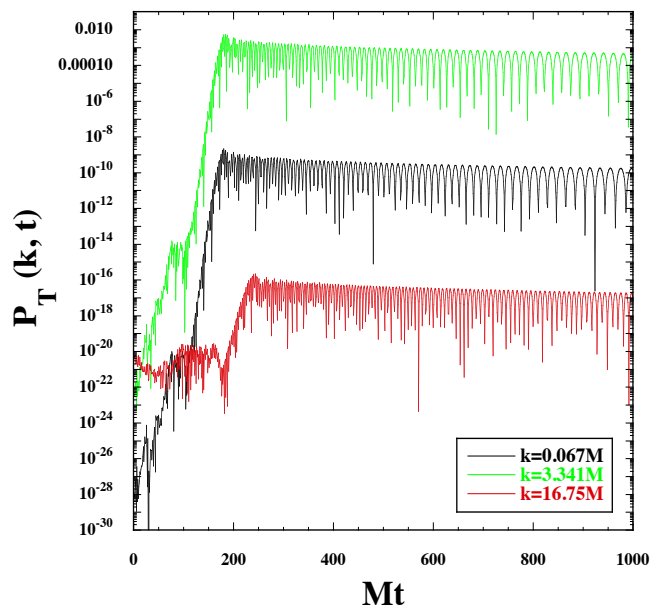


FIG. 5. Evolution of the tensor power spectrum during reheating in low-scale inflation with $M = 4.1 \times 10^{-11} M_{\text{pl}} = 10^8$ GeV for the tensor mass squared (2.13) with $\mu = 1.523 \times 10^4$. We integrate Eq. (3.13) from the onset of reheating ($a_i = 1$) with the initial conditions $\phi_i = \sqrt{2}M_{\text{pl}}$ and $\dot{\phi}_i = -\sqrt{2/3}MM_{\text{pl}}$. Each curve corresponds to the evolution of \mathcal{P}_T for $k = 0.067M$, $3.341M$, and $16.75M$, respectively.

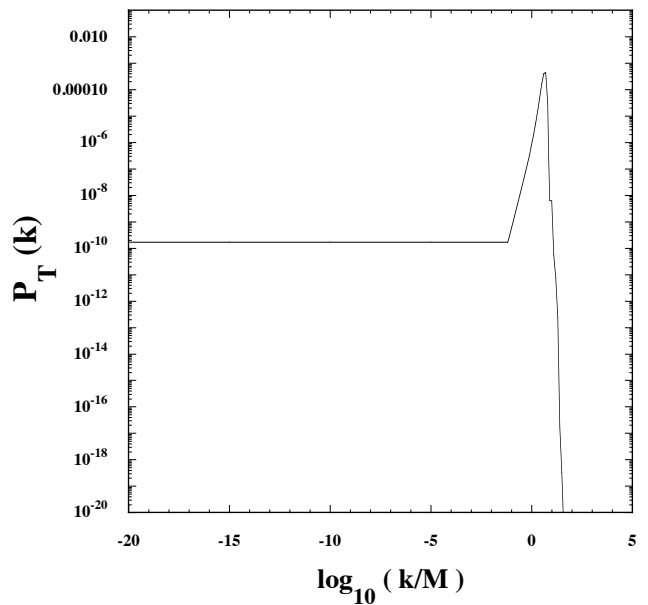


FIG. 6. The tensor power spectrum at $t = 10^3/M$ in low-scale inflation with the tensor mass squared (2.13) for the same model parameters used in Fig. 5.

radiation, so the effect of the tensor mass on the evolution of \mathcal{P}_T becomes negligible.

For the wavenumbers in the range $k_1 < k < k_2$, the power spectrum at $t = t_i$ is given by Eq. (3.30). Provided that the condition $k^2/a_i^2 \ll \mu\dot{\phi}_i^2/M_{\text{pl}}^2$ is satisfied, these modes are amplified by approximately the same factor as those in the range $k < k_1$. Hence the shape of the initial blue-tilted spectrum $\mathcal{P}_T(t_i) \propto k^3$ remains the same, and the resulting amplitude of GWs starts to increase for k larger than k_1 . Indeed, the numerical result given in Fig. 5 shows that the maximum value of \mathcal{P}_T reached for $k = 3.34M$ is larger than that for $k = k_1 = 0.067M$. For the wavenumber $k \gtrsim 10M$, the parametric excitation of GWs tends to be less efficient, see the evolution of \mathcal{P}_T for the mode $k = 16.75M$ in Fig. 5. The parametric resonance does not occur for the modes $k^2/a_i^2 > \mu\dot{\phi}_i^2/M_{\text{pl}}^2$, which translates to the condition $k \gtrsim k_{\text{cut}} \approx \sqrt{\mu}M \approx 10^2M$.

In Fig. 6, we plot the power spectrum $\mathcal{P}_T(k)$ at $t = 10^3/M$ for the same values of μ and M as those used in Fig. 5. As explained above, $\mathcal{P}_T(k)$ starts to increase for the modes $k > k_1 = 0.067M$ and it reaches the peak value around $k = 3.3M$. There is a sharp drop-down of $\mathcal{P}_T(k)$ for the modes $k \gtrsim 10M$. As we discussed in Sec. VB, the final amplitude of $\mathcal{P}_T(k)$ depends on the time when the inflaton decays to radiation. If the decay occurs earlier (later) than $t = 10^3/M$, the resulting amplitude of GWs tends to be larger (smaller) than $\mathcal{P}_T(k)$ shown in Fig. 6.

VII. SPECTRUM OF THE GRAVITATIONAL WAVE BACKGROUND

In this section, we compute the spectrum of the GW background generated in two models discussed in Secs. V and VI. The intensity of the GW background is conventionally defined as

$$\Omega_{\text{GW}} \equiv \frac{1}{\rho_c} \frac{d\rho_{\text{GW}}}{d \ln k}, \quad (7.1)$$

where $\rho_c = 3M_{\text{pl}}^2 H^2$ is the critical density of the Universe and ρ_{GW} is the energy density of GWs [38, 39]. The GW intensity can be expressed as [35, 40, 41]

$$\Omega_{\text{GW}}(k, t) = \frac{1}{12} \left(\frac{k}{aH} \right)^2 \mathcal{P}_T(k, t), \quad (7.2)$$

where $\mathcal{P}_T(k, t)$ is defined by Eq. (3.10).

After the inflaton decays to radiation at $t = t_\Gamma$, the GWs evolve as the standard massless tensor perturbation. For the modes outside the Hubble radius ($k < aH$) at time t_Γ , the tensor perturbation is frozen until the second horizon crossing (labelled by ‘‘sh’’). After the second horizon crossing, the GWs evolve as $v \propto a^{-1} e^{\pm ik\tau}$. Hence the present power spectrum $\mathcal{P}_T(k, t_0)$ is related to the one at time t_Γ , as

$$\mathcal{P}_T(k, t_0) = \mathcal{P}_T(k, t_\Gamma) \left(\frac{a_{\text{sh}}}{a_0} \right)^2, \quad (7.3)$$

where the subscript ‘‘0’’ denotes today’s value. In the Universe where the scale factor evolves as $a \propto t^p$, with p being a constant, the scale factor at the second horizon crossing has the k -dependence $a_{\text{sh}} \propto k^{p/(p-1)}$. For the primordial power spectrum $\mathcal{P}_T(k, t_\Gamma)$ with the spectral index \tilde{n}_t , i.e., $\mathcal{P}_T(k, t_\Gamma) \propto k^{\tilde{n}_t}$, today’s intensity (7.2) of the GW background has the k -dependence,

$$\Omega_{\text{GW}}(k, t_0) \propto k^{\tilde{n}_t + 2 + 2p/(p-1)}. \quad (7.4)$$

Hence $\Omega_{\text{GW}}(k, t_0) \propto k^{\tilde{n}_t}$ in the radiation era ($p = 1/2$) and $\Omega_{\text{GW}}(k, t_0) \propto k^{\tilde{n}_t - 2}$ in the matter era ($p = 2/3$). For $\tilde{n}_t = 0$, we have the scale-invariant spectrum $\Omega_{\text{GW}}(k, t_0) \propto k^0$ for $p = 1/2$ and the red-tilted spectrum $\Omega_{\text{GW}}(k, t_0) \propto k^{-2}$ for $p = 2/3$, respectively. The existence of peaks in $\mathcal{P}_T(k, t_\Gamma)$ seen in Figs. 4 and 6 should give rise to specific features in $\Omega_{\text{GW}}(k, t_0)$ (as we will discuss below).

The position of peaks in $\mathcal{P}_T(k, t_\Gamma)$ is related to the wavenumber $k_i = a_i H_i$ which crossed the Hubble radius at the end of inflation. Assuming that the entropy before the inflaton decay is conserved in the photon and neutrino background today (temperature T_0), the scale factor a_Γ at time t_Γ is given by [35, 42]

$$a_\Gamma = a_0 \left(\frac{11}{43} g_* \right)^{-1/3} \frac{T_0}{T_\Gamma}, \quad (7.5)$$

where T_Γ is the reheating temperature given by Eq. (4.7). During the time interval $t_i < t < t_\Gamma$, the energy density of the Universe decreases as $\rho \propto a^{-3}$, so we have $a_i = a_\Gamma (\rho_\Gamma / \rho_i)^{1/3}$, where $\rho_i \simeq 3M_{\text{pl}}^2 H_i^2$ and $\rho_\Gamma = \pi^2 g_* T_\Gamma^4 / 30$. On using the fact that today’s temperature is $T_0 \simeq 9.64 \times 10^{-32} M_{\text{pl}}$, the frequency $f_i = k_i / (2\pi) = a_i H_i / (2\pi)$ can be estimated as

$$\begin{aligned} f_i &\simeq 3.0 \times 10^{10} \left(\frac{g_*}{106.75} \right)^{-1/12} \left(\frac{H_i}{M_{\text{pl}}} \right)^{1/3} \left(\frac{\Gamma}{M_{\text{pl}}} \right)^{1/6} \text{ Hz} \\ &= 3.0 \times 10^{10} \left(\frac{g_*}{106.75} \right)^{-1/12} \left(\frac{H_i}{M_{\text{pl}}} \right)^{1/2} \left(\frac{\Gamma}{H_i} \right)^{1/6} \text{ Hz}. \end{aligned} \quad (7.6)$$

One observes that f_i can become very small and falls in the A-LIGO band for a very small H_i , say $H_i/M_{\text{pl}} \sim 10^{-18}$. In the following, we assume that the relativistic degree of freedom is equivalent to $g_* = 106.75$ at $t = t_\Gamma$.

A. Starobinsky inflation

In the Starobinsky model with the massless tensor, the tensor-to-scalar ratio r is of the order 10^{-3} at the CMB scale, which is much below the current observational bound ($r < 0.11$). On the other hand, the parametric resonance induced by the massive tensor may make it possible to detect the GWs in CMB measurements.

In Fig. 7, we plot today’s spectral energy density Ω_{GW} versus the frequency f in Starobinsky inflation with the

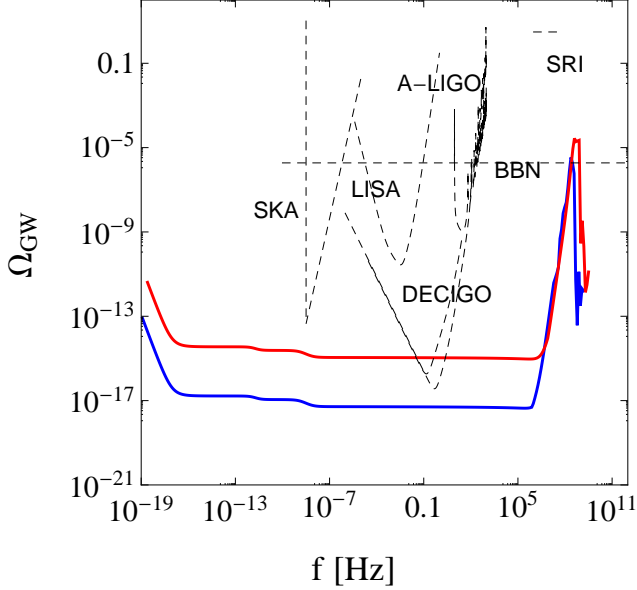


FIG. 7. Today's spectral energy density Ω_{GW} of the GW background versus the frequency $f = k/(2\pi)$ in the Starobinsky model with the ϕ -dependent tensor mass squared (2.12) for $M = 1.3 \times 10^{-5} M_{\text{pl}}$, $\lambda = 4.785 \times 10^{-7}$, $n = 2$, and $b = 2$. We also show the sensitivity curves for DECIGO [27], upgraded DECIGO [43], A-LIGO [26], LISA [44], SKA [45], and SRI [46], together with the upper bound from the BBN [47]. For a recent BBN status report, see, e.g., Ref. [48]. Each line corresponds to the case in which the inflaton decay to the radiation occurs at $t = 10^2/M$ (red) and $t = 10^4/M$ (blue).

ϕ -dependent tensor mass squared (2.12) for $M = 1.3 \times 10^{-5} M_{\text{pl}}$, $\lambda = 4.785 \times 10^{-7}$, $n = 2$, and $b = 2$. In this case, the tensor power spectrum \mathcal{P}_T relevant to the CMB grows to the amplitude 7×10^{-10} around the time $t = 10^2/M$. The top (red) line in Fig. 7 corresponds to the case in which the inflaton decays to the radiation at time $t = 10^2/M$. The decay constant in this case is given by $\Gamma = 10^{-2}M$ with $H_i \simeq 0.3M$, so we have $f_i \simeq 3 \times 10^7$ Hz from Eq. (7.6). Since the primordial spectrum $\mathcal{P}_T(k)$ at $t = 10^2/M$ has a peak around $k = 40k_i$, this structure is inherited to $\Omega_{\text{GW}}(f, t_0)$ with the peak around the frequency $f = 40f_i \simeq 10^9$ Hz.

Although the peak position of $\Omega_{\text{GW}}(f, t_0)$ is at a frequency much higher than the ranges relevant to the detection sensitivities of A-LIGO and DECIGO, we find there is a range of frequencies around $f = 0.1$ Hz in which the theoretical line is within the DECIGO detection range. The GWs around $f = 0.1$ Hz are the ones from the nearly scale-invariant primordial perturbations whose horizon re-entry occurs in the radiation era, so $\Omega_{\text{GW}}(f, t_0)$ is almost scale-invariant around those frequencies.

For the decay constant $\Gamma = 10^{-2}M$, the maximum

value of $\Omega_{\text{GW}}(f, t_0)$ exceeds the upper bound constrained from the Big Bang Nucleosynthesis (BBN) [47]. In the following, we will explain how the BBN places bounds on the GW amplitude in considerable detail. Neutrinos contribute to the energy density of radiation, and their energy density is written using the effective number of neutrinos N_{eff}^ν as $\rho_\nu = (7/8)(4/11)^{4/3} N_{\text{eff}}^\nu \rho_\gamma$, where ρ_γ is the energy density of photons. The GW contribution to the radiation energy density at the time of BBN can be effectively described by $N_{\text{eff}} = N_{\text{eff}}^\nu + N_{\text{eff}}^{\text{GW}}$ with

$$\begin{aligned} N_{\text{eff}}^{\text{GW}} &= \frac{8}{7} \left(\frac{g_{*,s}(T = 1 \text{ MeV})}{g_{*,s}(T_0)} \right)^{4/3} \frac{\rho_{\text{GW},0}}{\rho_{\gamma,0}} \\ &= \frac{h^2}{5.6 \times 10^{-6}} \int d(\ln f) \Omega_{\text{GW}}(f), \end{aligned} \quad (7.7)$$

where $g_{*,s}$ is the effective number of degrees of freedom for entropy and we adopted the standard values $g_{*,s}(T_0) = 3.91$ and $g_{*,s}(T = 1 \text{ MeV}) = 10.75$. In the second step, we have used the definition of Ω_{GW} in Eq. (7.1) and today's density parameter of photons $\Omega_{\gamma,0} = \rho_{\gamma,0}/(3M_{\text{pl}}^2 H_0^2) \simeq 2.47 \times 10^{-5} h^{-2}$, where $H_0 = 100 h \text{ km s}^{-1} \text{ Mpc}^{-1}$ is today's Hubble expansion rate. Thus, using the upper limit $N_{\text{eff}} < 3.2$ and the standard prediction of the effective number of neutrinos $N_{\text{eff}}^\nu = 3.045$ [49], we can obtain the upper limit on the GW amplitude as [39, 47]

$$\begin{aligned} \int_{10^{-10} \text{ Hz}}^{10^{10} \text{ Hz}} d(\ln f) \Omega_{\text{GW}}(f) &< \frac{5.6 \times 10^{-6}}{h^2} (N_{\text{eff}} - N_{\text{eff}}^\nu) \\ &< 1.9 \times 10^{-6}, \end{aligned} \quad (7.8)$$

where the reduced Hubble constant $h \simeq 0.6763$ [50] has been used in the second line.

For smaller Γ , the overall amplitude of $\Omega_{\text{GW}}(f, t_0)$ decreases with the shift of the peak position toward smaller frequencies, see the blue line in Fig. 7 for the decay constant $\Gamma = 10^{-4}M$. Provided that $\Gamma < 10^{-4}M$, the model with the coupling $\lambda = 4.785 \times 10^{-7}$ is within the BBN bound. For such a decay constant, the theoretical line is below the sensitivity region of DECIGO. For smaller λ the parametric resonance is less efficient, so the resulting amplitude of $\Omega_{\text{GW}}(f, t_0)$ gets smaller. In such cases, the BBN constraint can be satisfied for larger Γ . However, to satisfy the BBN bound, the model with $n = 2$ and $b = 2$ seems to predict the value of $\Omega_{\text{GW}}(f, t_0)$ too small to be in the DECIGO sensitivity region. There may be some cases with different values of n and b in which the theoretical line is within the DECIGO detection range while satisfying the BBN bound, but the parametric resonance is typically too efficient to give rise to a sharp peak which overshoots the BBN upper limit.

B. Low-scale inflation

In low-scale inflation discussed in Sec. VI, the tensor power spectrum relevant to CMB measurements is

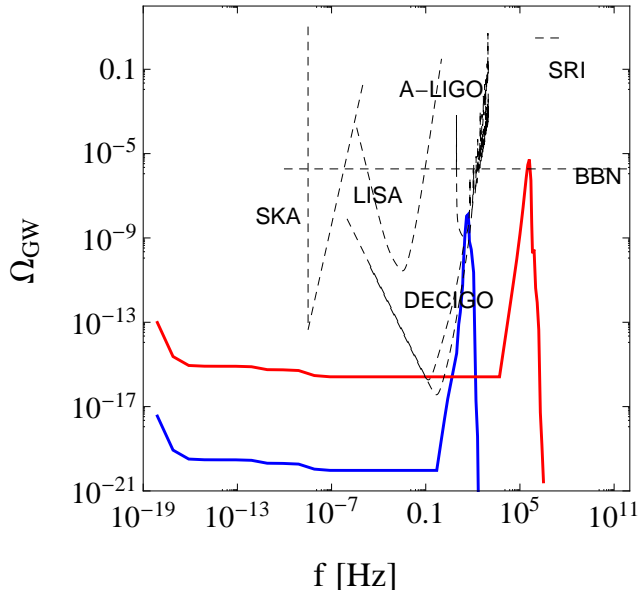


FIG. 8. Ω_{GW} versus f in low-scale inflation with the ϕ -dependent tensor mass squared (2.13). The sensitivity curves of GW experiments are the same as shown in Fig. 7. Each line corresponds to the models with (i) $M = 10^8$ GeV, $\mu = 1.523 \times 10^4$, $k_1 = 0.067M$, $t_\Gamma = 10^3/M$ (red), and (ii) $M = 1$ GeV, $\mu = 4.78 \times 10^4$, $k_1 = 0.067M$, $t_\Gamma = 10^3/M$ (blue).

very small at the end of inflation, but the parametric resonance driven by the tensor mass squared (2.13) can amplify the GWs to \mathcal{P}_T larger than 10^{-10} . Moreover, since the Hubble parameter H_i at the onset of reheating and the decay constant Γ are much smaller than those in Starobinsky inflation, the frequency f_i relevant to the peak position of Ω_{GW} shifts toward smaller values.

In Fig. 8, we plot today's GW background spectrum $\Omega_{\text{GW}}(f, t_0)$ for $M = 10^8$ GeV and $\Gamma = 10^{-3}M$ with the coupling $\mu = 1.523 \times 10^4$ (red line), which are the same model parameters as those for Figs. 5 and 6. For $H_i \simeq 2M/3$ as estimated in Eq. (6.2), the frequency formula (7.6) gives $f_i \simeq 5 \times 10^4$ Hz. Since the peak wavenumber of $\mathcal{P}_T(k)$ shown in Fig. 6 is $k \simeq 5k_i$, the associated frequency at the maximum of $\Omega_{\text{GW}}(f, t_0)$ is given by $f = \mathcal{O}(10^5)$ Hz. In this case, the peak amplitude is marginally consistent with the BBN bound. The peak position is outside the detection range of the current ground-based GW measurements, but the predicted amplitude reaches the sensitivity curve of DECIGO around the frequency $f = 0.1$ Hz.

There is a proposed detector design called the Synchronous Recycling Interferometer (SRI) [46] aiming to detect GWs at high frequencies around 10^6 Hz $< f < 10^8$ Hz. If the SRI reaches the sensitivity region below the BBN bound plotted in Fig. 8, then we have the pos-

sibility to test our massive gravity scenario in low-scale inflation with 10^8 GeV $\lesssim M \lesssim 10^{12}$ GeV.

In Fig. 8, we also show $\Omega_{\text{GW}}(f, t_0)$ for $M = 1$ GeV and $\Gamma = 10^{-3}M$ with the coupling $\mu = 4.78 \times 10^4$ (blue line). In this case, the frequency formula (7.6) gives $f_i \simeq 5$ Hz with the peak wavenumber $k \simeq 5k_i$. This means that the spectrum is peaked at the frequency $f = \mathcal{O}(10)$ Hz. For the coupling μ used in Fig. 8, the maximum value of $\Omega_{\text{GW}}(f, t_0)$ is 1.3×10^{-8} at $f = 50.2$ Hz, which satisfies the latest A-LIGO bound $\Omega_{\text{GW}}(f, t_0) < 1.7 \times 10^{-7}$ in the band $20 \text{ Hz} < f < 86 \text{ Hz}$ [51]. This case is within the sensitivity region of the A-LIGO measurement. Thus there is a possibility for detecting the primordial GWs in the near future. The theoretical line is also on the verge of the DECIGO sensitivity curve. For increasing μ the amplitude of $\Omega_{\text{GW}}(f, t_0)$ gets larger, so the present A-LIGO measurement places the upper bound $\mu \lesssim 5 \times 10^4$ for $M = 1$ GeV. Thus, in low-scale inflation with $M = \mathcal{O}(1)$ GeV, it is possible to probe the physics of the massive tensor modes in direct GW measurements.

VIII. CONCLUSIONS

In this paper, we studied the signature of the massive gravity theory in which the oscillating tensor mass during reheating after inflation gives rise to the parametric amplification of the primordial tensor perturbation. For the theory described by the action (2.6), the vector modes do not propagate due to the internal symmetry (2.7). As a result, we are left with one scalar and two tensor propagating degrees of freedom with a time-dependent tensor mass. We identify the scalar degree of freedom as an inflaton field.

For the broad parametric resonance to occur during reheating, the tensor mass m_g needs to be much larger than the Hubble expansion rate H . On the other hand, we require the condition $m_g^2 \ll H^2$ to avoid the strong suppression of massive GWs in the preceding inflationary epoch. This was made possible in our Lorentz-violating theory because it is free from the Higuchi bound, $m_g^2 > 2H^2$ [22]. We proposed two explicit forms of m_g^2 satisfying these two requirements, see Eqs. (2.12) and (2.13). These requirements imply the existence of a transition from the regime $m_g^2 \lesssim H^2$ to the regime $m_g^2 \gtrsim H^2$ around the end of inflation.

In Sec. III, we analytically estimated the tensor power spectrum $\mathcal{P}_T(k)$ at onset of reheating by considering the transition of m_g^2 during inflation. In Sec. IV, we derived conditions for the occurrence of parametric resonance and typical wavenumbers k associated with the amplification of GWs.

In Sec. V, we considered the Starobinsky model with the ϕ -dependent tensor mass squared (2.12) and numerically computed $\mathcal{P}_T(k)$ both at the onset and end of the amplification stage. As we see in Fig. 2, the large-scale GWs relevant to CMB observations have a nearly scale-invariant spectrum at the end of inflation, whereas

the small-scale modes which were inside the Hubble radius during reheating have a highly blue-tilted spectrum. The parametric resonance leads to the amplification of GWs up to a cutoff wavenumber, Eq. (4.15) (see Fig. 3). The resulting power spectrum $\mathcal{P}_T(k)$, which is plotted in Fig. 4, has a sharp peak around the wavenumber $k = \mathcal{O}(10)k_i$. For the modes satisfying the condition $k^2/a^2 < m_g^2$, the amplitude of GWs decreases as $\langle \mathcal{P}_T \rangle \propto t^{-1}$ after reaching its maximum. This decrease continues until the time t_Γ at which the inflaton decays to radiation. For $t > t_\Gamma$, the tensor perturbation behaves as in the standard massless case. Thus the final amplitude of the GW spectrum varies with the time t_Γ . The later the time t_Γ is, the smaller the amplitude becomes.

In Sec. VI, we studied low-scale inflation with the $\dot{\phi}$ -dependent tensor mass squared (2.13). We considered a scenario in which the slow-roll parameter ϵ relevant to the CMB observations is much smaller than 10^{-4} and assumed a rapid transition to the potential $V(\phi) = M^2\phi^2/2$, Eq. (6.1), to occur around $\phi \approx M_{\text{pl}}$. In such models, the power spectrum \mathcal{P}_T at the beginning of reheating is very small, but the parametric resonance driven by the massive tensor can amplify GWs to the detectable level of CMB observations (see Fig. 5 for the case $M = 10^8$ GeV). This mechanism is at work even for very low-scale inflation with the mass like $M = 1$ GeV. The GWs can be efficiently amplified up to the wavenumber k_{cut} of order $10k_i$ where $\mathcal{P}_T(k, \tau_\Gamma)$ is peaked (see Fig. 6).

We note that, in a low-scale inflationary scenario where the transition to the potential $V(\phi) = M^2\phi^2/2$ occurs for ϕ much smaller than M_{pl} , the parametric resonance tends to be less efficient relative to the model studied in our paper for the same coupling constant μ . On the other hand, if we consider a much larger μ , one may be able to make the parametric resonance efficient again. However, this will rather generally lead to extremely strong suppression during inflation unless one fine-tunes the behavior of $\dot{\phi}^2$ near the end of inflation. Such a case may be possible in models with a waterfall transition, but it is beyond the scope of the present paper.

In Sec. VII, we computed today's energy density spectrum $\Omega_{\text{GW}}(f, t_0)$ of the GW background in both Starobinsky inflation and low-scale inflation. The peak frequency f_i of $\Omega_{\text{GW}}(f, t_0)$ is given by the formula (7.6).

In the Starobinsky model, the peak is at around $f = 10^9$ Hz, which is much larger than the frequencies relevant to the current direct GW measurements (see Fig. 7). There is a range of frequencies around $f = 0.1$ Hz in which the massive gravity scenario in Starobinsky inflation can reach the sensitivity curves of DECIGO and upgraded DECIGO, but the BBN bound is quite tight to limit the significant amplification of GWs during preheating.

Before concluding the paper, let us recapitulate a couple of intriguing possibilities. One is the case of very low-scale inflation. Since H_i and Γ in low-scale inflation can be much smaller than those in Starobinsky inflation, the peak of $\Omega_{\text{GW}}(f, t_0)$ may appear at a much lower frequency. For the model parameters $M = 1$ GeV and $\Gamma = 10^{-3}M$, the peak of $\Omega_{\text{GW}}(f, t_0)$ reaches the sensitivity curve of A-LIGO, see Fig. 8.

The other is the possibility of high frequency GW observations. If a future high frequency (10^6 Hz $< f < 10^8$ Hz) GW detector like SRI can improve the sensitivity below the BBN bound, it will offer the possibility for testing our massive gravity scenario in low-scale inflation with 10^8 GeV $\lesssim M \lesssim 10^{12}$ GeV.

In conclusion, what is really exciting is that the existence of the time-dependent tensor mass in the early Universe can be potentially probed not only by CMB measurements but also by direct GW measurements at many different frequencies. Thus our massive gravity model provides an ideal target for the multi-frequency gravitational wave astronomy in years to come.

ACKNOWLEDGMENTS

This work is supported in part by the MEXT KAKENHI No.15H05888. SK is supported by the Career Development Project for Researchers of Allied Universities, and by JSPS Grant-in-Aid for Scientific Research No.17K14282. CL is supported by JSPS postdoc fellowship for overseas researchers, and by JSPS Grant-in-Aid for Scientific Research No.15F15321. ST is supported by JSPS Grant-in-Aid for Scientific Research No. 24540286 and MEXT KAKENHI Grant-in-Aid for Scientific Research on Innovative Areas ‘‘Cosmic Acceleration’’ (No. 15H05890).

-
- [1] A. A. Starobinsky, Phys. Lett. B **91**, 99 (1980).
 [2] R. Brout, F. Englert and E. Gunzig, Annals Phys. **115**, 78 (1978); D. Kazanas, Astrophys. J. **241** L59 (1980); K. Sato, Mon. Not. R. Astron. Soc. **195**, 467 (1981); Phys. Lett. **99B**, 66 (1981); A. H. Guth, Phys. Rev. D **23**, 347 (1981).
 [3] V. F. Mukhanov and G. V. Chibisov, JETP Lett. **33**, 532 (1981).
 [4] A. H. Guth and S. Y. Pi, Phys. Rev. Lett. **49** (1982) 1110; S. W. Hawking, Phys. Lett. B **115**, 295 (1982);

- A. A. Starobinsky, Phys. Lett. B **117** (1982) 175; J. M. Bardeen, P. J. Steinhardt and M. S. Turner, Phys. Rev. D **28**, 679 (1983).
 [5] H. Kodama and M. Sasaki, Prog. Theor. Phys. Suppl. **78**, 1 (1984); V. F. Mukhanov, JETP Lett. **41**, 493 (1985) [Pisma Zh. Eksp. Teor. Fiz. **41**, 402 (1985)]; M. Sasaki, Prog. Theor. Phys. **76**, 1036 (1986); V. F. Mukhanov, H. A. Feldman and R. H. Brandenberger, Phys. Rept. **215**, 203 (1992).

- [6] P. A. R. Ade *et al.* [Planck Collaboration], *Astron. Astrophys.* **594**, A20 (2016) [arXiv:1502.02114 [astro-ph.CO]].
- [7] A. A. Starobinsky, *JETP Lett.* **30**, 682 (1979) [*Pisma Zh. Eksp. Teor. Fiz.* **30**, 719 (1979)].
- [8] J. E. Lidsey, A. R. Liddle, E. W. Kolb, E. J. Copeland, *Rev. Mod. Phys.* **69**, 373 (1997); D. H. Lyth and A. Riotto, *Phys. Rept.* **314**, 1 (1999); B. A. Bassett, S. Tsujikawa and D. Wands, *Rev. Mod. Phys.* **78**, 537 (2006).
- [9] D. H. Lyth, *Phys. Rev. Lett.* **78**, 1861 (1997).
- [10] D. Baumann and L. McAllister, *Phys. Rev. D* **75**, 123508 (2007) [hep-th/0610285].
- [11] S. Tsujikawa, *PTEP* **2014**, no. 6, 06B104 (2014) [arXiv:1401.4688 [astro-ph.CO]].
- [12] A. De Felice and S. Tsujikawa, *Living Rev. Rel.* **13**, 3 (2010) [arXiv:1002.4928 [gr-qc]].
- [13] M. Hazumi *et al.* (LiteBIRD), *Proc. SPIE Int. Soc. Opt. Eng.* **8442**, 844219 (2012).
- [14] K. N. Abazajian *et al.* [CMB-S4 Collaboration], arXiv:1610.02743 [astro-ph.CO].
- [15] S. Kachru, R. Kallosh, A. D. Linde, J. M. Maldacena, L. P. McAllister and S. P. Trivedi, *JCAP* **0310**, 013 (2003) [hep-th/0308055]; D. Baumann, A. Dymarsky, I. R. Klebanov, J. M. Maldacena, L. P. McAllister and A. Murugan, *JHEP* **0611**, 031 (2006) [hep-th/0607050]; S. Panda, M. Sami and S. Tsujikawa, *Phys. Rev. D* **76**, 103512 (2007) [arXiv:0707.2848 [hep-th]]; D. Baumann and L. McAllister, arXiv:1404.2601 [hep-th].
- [16] C. Lin and M. Sasaki, *Phys. Lett. B* **752**, 84 (2016) [arXiv:1504.01373 [astro-ph.CO]].
- [17] S. Y. Khlebnikov and I. I. Tkachev, *Phys. Rev. D* **56**, 653 (1997) [hep-ph/9701423]; J. Garcia-Bellido and D. G. Figueroa, *Phys. Rev. Lett.* **98**, 061302 (2007) [astro-ph/0701014]; J. Garcia-Bellido, D. G. Figueroa and A. Sastre, *Phys. Rev. D* **77**, 043517 (2008) [arXiv:0707.0839 [hep-ph]].
- [18] S. L. Dubovsky, *JHEP* **0410**, 076 (2004) [hep-th/0409124].
- [19] S. L. Dubovsky, P. G. Tinyakov and I. I. Tkachev, *Phys. Rev. Lett.* **94**, 181102 (2005) [hep-th/0411158].
- [20] M. Fierz and W. Pauli, *Proc. Roy. Soc. Lond.* **A173**, 211-232 (1939).
- [21] C. de Rham, G. Gabadadze and A. J. Tolley, *Phys. Rev. Lett.* **106**, 231101 (2011) [arXiv:1011.1232 [hep-th]].
- [22] A. Higuchi, *Nucl. Phys. B* **282**, 397 (1987).
- [23] G. Domenech, T. Hiramatsu, C. Lin, M. Sasaki, M. Shiraishi and Y. Wang, *JCAP* **1705**, no. 05, 034 (2017) [arXiv:1701.05554 [astro-ph.CO]].
- [24] L. Kofman, A. D. Linde and A. A. Starobinsky, *Phys. Rev. Lett.* **73**, 3195 (1994) [hep-th/9405187].
- [25] L. Kofman, A. D. Linde and A. A. Starobinsky, *Phys. Rev. D* **56**, 3258 (1997) [hep-ph/9704452].
- [26] B. P. Abbott *et al.* [LIGO Scientific and Virgo Collaborations], *Phys. Rev. Lett.* **116**, 061102 (2016) [arXiv:1602.03837 [gr-qc]]; B. P. Abbott *et al.* [LIGO Scientific and Virgo Collaborations], *Phys. Rev. Lett.* **116**, no. 24, 241103 (2016) [arXiv:1606.04855 [gr-qc]].
- [27] N. Seto, S. Kawamura and T. Nakamura, *Phys. Rev. Lett.* **87**, 221103 (2001) [astro-ph/0108011]; S. Kawamura *et al.*, *Class. Quant. Grav.* **23**, S125 (2006); S. Kawamura *et al.*, *Class. Quant. Grav.* **28**, 094011 (2011).
- [28] C. Lin and L. Z. Labun, *JHEP* **1603**, 128 (2016) [arXiv:1501.07160 [hep-th]].
- [29] K. Jedamzik and G. Sigl, *Phys. Rev. D* **61**, 023519 (2000) [hep-ph/9906287]; P. Ivanov, *Phys. Rev. D* **61**, 023505 (2000) [astro-ph/9906415]; A. R. Liddle, D. H. Lyth, K. A. Malik and D. Wands, *Phys. Rev. D* **61**, 103509 (2000) [hep-ph/9912473]; C. Gordon, D. Wands, B. A. Bassett and R. Maartens, *Phys. Rev. D* **63**, 023506 (2001) [astro-ph/0009131]; S. Tsujikawa and B. A. Bassett, *Phys. Lett. B* **536**, 9 (2002) [astro-ph/0204031].
- [30] C. de Rham, J. T. Deskins, A. J. Tolley and S. Y. Zhou, *Rev. Mod. Phys.* **89**, no. 2, 025004 (2017) [arXiv:1606.08462 [astro-ph.CO]].
- [31] A. D. Linde, *Phys. Lett.* **129B**, 177 (1983).
- [32] R. Kallosh and A. Linde, *JCAP* **1310**, 033 (2013) [arXiv:1307.7938 [hep-th]].
- [33] A. Albrecht, P. J. Steinhardt, M. S. Turner and F. Wilczek, *Phys. Rev. Lett.* **48**, 1437 (1982); A. D. Dolgov and A. D. Linde, *Phys. Lett. B* **116**, 329 (1982); L. F. Abbott, E. Farhi and M. B. Wise, *Phys. Lett. B* **117**, 29 (1982).
- [34] A. D. Dolgov and A. D. Linde, *Phys. Lett. B* **116**, 329 (1982); L. F. Abbott, E. Farhi and M. B. Wise, *Phys. Lett. B* **117**, 29 (1982).
- [35] S. Kuroyanagi, S. Tsujikawa, T. Chiba and N. Sugiyama, *Phys. Rev. D* **90**, 063513 (2014) [arXiv:1406.1369 [astro-ph.CO]].
- [36] S. Tsujikawa, K. i. Maeda and T. Torii, *Phys. Rev. D* **60**, 063515 (1999) [hep-ph/9901306].
- [37] S. Kuroyanagi, T. Chiba and N. Sugiyama, *Phys. Rev. D* **79**, 103501 (2009) [arXiv:0804.3249 [astro-ph]].
- [38] B. Allen and J. D. Romano, *Phys. Rev. D* **59**, 102001 (1999) [gr-qc/9710117].
- [39] M. Maggiore, *Phys. Rept.* **331**, 283 (2000) [gr-qc/9909001].
- [40] K. Nakayama, S. Saito, Y. Suwa, and J. Yokoyama, *Phys. Rev. D* **77**, 124001 (2008). [arXiv:0802.2452 [hep-ph]]; *JCAP* **0806**, 020 (2008) [arXiv:0804.1827 [astro-ph]].
- [41] S. Kuroyanagi, T. Chiba and N. Sugiyama, *Phys. Rev. D* **83**, 043514 (2011) [arXiv:1010.5246 [astro-ph.CO]].
- [42] L. Dai, M. Kamionkowski and J. Wang, *Phys. Rev. Lett.* **113**, 041302 (2014) [arXiv:1404.6704 [astro-ph.CO]].
- [43] K. Yagi and N. Seto, *Phys. Rev. D* **83**, 044011 (2011) [arXiv:1101.3940 [astro-ph.CO]].
- [44] P. Amaro-Seoane *et al.*, *Class. Quant. Grav.* **29**, 124016 (2012) [arXiv:1202.0839 [gr-qc]].
- [45] G. Janssen *et al.*, *PoS AASKA* **14**, 037 (2015) [arXiv:1501.00127 [astro-ph.IM]].
- [46] A. Nishizawa *et al.*, *Phys. Rev. D* **77**, 022002 (2008) [arXiv:0710.1944 [gr-qc]]. A. Nishizawa *et al.*, *Class. Quant. Grav.* **25**, 225011 (2008) [arXiv:0801.4149 [gr-qc]].
- [47] G. Cabass, L. Pagano, L. Salvati, M. Gerbino, E. Giusarma and A. Melchiorri, *Phys. Rev. D* **93**, 063508 (2016) [arXiv:1511.05146 [astro-ph.CO]].
- [48] R. H. Cyburt, B. D. Fields, K. A. Olive and T. H. Yeh, *Rev. Mod. Phys.* **88**, 015004 (2016) [arXiv:1505.01076 [astro-ph.CO]].
- [49] P. F. de Salas, S. Gariazzo, J. Lesgourgues and S. Pastor, *JCAP* **1709**, no. 09, 034 (2017) [arXiv:1706.09850 [astro-ph.CO]].
- [50] P. A. R. Ade *et al.* [Planck Collaboration], *Astron. Astrophys.* **594**, A13 (2016) [arXiv:1502.01589 [astro-ph.CO]].
- [51] B. P. Abbott *et al.* [LIGO Scientific and Virgo Collaborations], *Phys. Rev. Lett.* **118**, no. 12, 121101 (2017) [arXiv:1612.02029 [gr-qc]].